# REPORT DOCUMENTATION PAGE

Form Approved OMB NO. 0704-0188



| 1. REPORT DATE (DD-MM-YYYY) | 2. REPORT TYPE | 3. DATES COVERED (From - To) |
|---|---|---|
| 26-08-2013 | Final Report | 1-Sep-2010 - 31-Aug-2014 |

4. TITLE AND SUBTITLE

High Throughput via Cross-Layer Interference Alignment for Mobile Ad Hoc Networks

5a. CONTRACT NUMBER
W911NF-10-1-0420

5b. GRANT NUMBER

5c. PROGRAM ELEMENT NUMBER
611102

6. AUTHORS

Robert W. Heath Jr.

5d. PROJECT NUMBER

5e. TASK NUMBER

5f. WORK UNIT NUMBER

7. PERFORMING ORGANIZATION NAMES AND ADDRESSES

University of Texas at Austin
101 East 27th Street
Suite 5.300
Austin, TX 78712 -1539

8. PERFORMING ORGANIZATION REPORT NUMBER

9. SPONSORING/MONITORING AGENCY NAME(S) AND ADDRESS(ES)

U.S. Army Research Office
P.O. Box 12211
Research Triangle Park, NC 27709-2211

10. SPONSOR/MONITOR'S ACRONYM(S)
ARO

11. SPONSOR/MONITOR'S REPORT NUMBER(S)
58082-NS.16

12. DISTRIBUTION AVAILIBILITY STATEMENT

Approved for Public Release; Distribution Unlimited

13. SUPPLEMENTARY NOTES

The views, opinions and/or findings contained in this report are those of the author(s) and should not contrued as an official Department of the Army position, policy or decision, unless so designated by other documentation.

14. ABSTRACT

Recent investigations into the fundamental limits of mobile ad hoc networks have produced a physical layer method for approaching their capacity. This strategy, known as interference alignment, requires cooperation, rather than competition, among the transceivers in the network. Under ideal circumstances, every user can achieve reliable communication at rates approaching one half of the interference-free capacity. Unfortunately, prior research on interference alignment makes many assumptions that make it difficult to realize interference alignment in practice.

15. SUBJECT TERMS

wireless communications, interference, interference alignment

| 16. SECURITY CLASSIFICATION OF: | | | 17. LIMITATION OF ABSTRACT | 15. NUMBER OF PAGES | 19a. NAME OF RESPONSIBLE PERSON |
|---|---|---|---|---|---|
| a. REPORT | b. ABSTRACT | c. THIS PAGE | | | Robert Heath, Jr. |
| UU | UU | UU | UU | | 19b. TELEPHONE NUMBER 512-232-2014 |

**Report Title**

High Throughput via Cross-Layer Interference Alignment for Mobile Ad Hoc Networks


**ABSTRACT**

Recent investigations into the fundamental limits of mobile ad hoc networks have produced a physical layer method for approaching their capacity. This strategy, known as interference alignment, requires cooperation, rather than competition, among the transceivers in the network. Under ideal circumstances, every user can achieve reliable communication at rates approaching one half of the interference-free capacity. Unfortunately, prior research on interference alignment makes many assumptions that make it difficult to realize interference alignment in practice. This report summarizes the PI's work on realizing interference alignment in multiple-input multiple-output (MIMO) communication channels. The emphasis is on networks where clusters of users cooperate together, since this provides a good balance between network overhead and performance. One contribution was to devise a way to add new users to an existing cluster of interference aligned users. Different algorithms were devised as a function of the number of antennas in the network. Another contribution was to analyze interference alignment in a network with random clusters of users. The cases where interference alignment was preferred to other simpler communication strategies was characterized. Another contribution was to determine the impact of distributing the antennas. It was found that distributed antennas lead to higher performance with interference alignment, and new algorithms were designed to achieve that performance. A final contribution was to prototype an interference alignment network. A distributed prototype was constructed with over-the-air synchronization and feedback, demonstrating the viability of interference alignment for small networks in practice.


---

## Enter List of papers submitted or published that acknowledge ARO support from the start of the project to the date of this printing. List the papers, including journal references, in the following categories:

### (a) Papers published in peer-reviewed journals (N/A for none)

| Received | | Paper |
|---|---|---|
| 08/26/2013 | 14.00 | Angel Lozano, Robert W. Heath, Nachiappan Valliappan. Antenna Subset Modulation for Secure Millimeter-Wave Wireless Communication, IEEE Transactions on Communications, (08 2013): 0. doi: 10.1109/TCOMM.2013.061013.120459 |
| 09/04/2012 | 5.00 | Jeffrey G. Andrews, Robert W. Heath, Behrang Nosrat-Makouei. User Arrival in MIMO Interference Alignment Networks, IEEE Transactions on Wireless Communications, (02 2012): 0. doi: 10.1109/TWC.2011.120511.111088 |
| **TOTAL:** | **2** | |

**Number of Papers published in peer-reviewed journals:**

---

### (b) Papers published in non-peer-reviewed journals (N/A for none)

| Received | | Paper |
|---|---|---|
| **TOTAL:** | | |

**Number of Papers published in non peer-reviewed journals:**

## (c) Presentations

**Number of Presentations:** 0.00

## Non Peer-Reviewed Conference Proceeding publications (other than abstracts):

| Received | | Paper |
|---|---|---|
| 01/30/2013 | 12.00 | Jonathan Starr, Seogoo Lee, Jackson Massey, Dongwook Lee, Andreas Gerstlauer, Robert Heath. Implementation of a Real-Time WirelessInterference Alignment Network, Asilomar Conference on Signals, Systems, and Computers. 2012/11/05 01:00:00, . : , |
| **TOTAL:** | **1** | |

**Number of Non Peer-Reviewed Conference Proceeding publications (other than abstracts):**

## Peer-Reviewed Conference Proceeding publications (other than abstracts):

| Received | | Paper |
|---|---|---|
| 08/31/2011 | 1.00 | Jeffrey G. Andrews, Robert W. Heath, Behrang Nosrat-Makouei. User admission in MIMO interference alignment networks, ICASSP 2011 - 2011 IEEE International Conference on Acoustics, Speech and Signal Processing (ICASSP). 2011/05/21 18:00:00, Prague, Czech Republic. : , |
| 09/04/2012 | 4.00 | Behrang Nosrat-Makouei, Jeffrey G. Andrews, Robert W. Heath, Radha Krishna Ganti. MIMO interference alignment in random access networks, 2011 45th Asilomar Conference on Signals, Systems and Computers. 2011/11/05 01:00:00, Pacific Grove, CA, USA. : , |
| **TOTAL:** | **2** | |

**Number of Peer-Reviewed Conference Proceeding publications (other than abstracts):**

## (d) Manuscripts

| Received | | Paper |
|---|---|---|
| 01/30/2013 | 9.00 | Namyoon Lee, Robert Heath. Multi-Way Information Exchange OverCompletely-Connected Interference Networkswith a Multi-Antenna Relau, IEEE Transactions on Information Theory (02 2013) |
| 01/30/2013 | 11.00 | Namyoon Lee, Robert Heath. Degrees of Freedom for the Two-Cell Two-HopMIMO Interference Channel: Interference-FreeRelay Transmission and Spectrally EfficientRelaying Protocol, IEEE TRANSACTIONS ON INFORMATION THEORY (11 2011) |
| 01/30/2013 | 10.00 | Namyoon Lee, Robert Heath. Space-Time Interference Alignment andDegrees of Freedom Regions for the MISOBroadcast Channel with Periodic CSI Feedback, IEEE Transactions on Information Theory (04 2012) |
| 08/26/2013 | 15.00 | Omar El Ayach, Robert W. Heath Jr., Jonathan Starr. Interference Alignment in Distributed AntennaSystems, IEEE Trans. Wireless Communication (04 2013) |
| 09/04/2012 | 7.00 | Behrang Nosrat Makouei, Radha Krishna Ganti, Jeffrey G. Andrews, Robert W. Heath Jr.. MIMO Interference Alignment in Random Access Networks, IEEE Transactions on Communications (07 2012) |
| **TOTAL:** | **5** | |

**Number of Manuscripts:**

---

## Books

| Received | Paper |
|---|---|
| **TOTAL:** | |

## Patents Submitted

---

## Patents Awarded

---

## Awards

---

## Graduate Students

| NAME | PERCENT_SUPPORTED | Discipline |
|---|---|---|
| Omar El Ayach | 0.33 | |
| Nachiappan Valliappan | 0.10 | |
| Namyoon Lee | 0.18 | |
| Berhang Nosrat Makouei | 0.66 | |
| Jonathan Starr | 0.18 | |
| Jackson Massey | 0.24 | |
| **FTE Equivalent:** | **1.69** | |
| **Total Number:** | **6** | |

## Names of Post Doctorates

| NAME | PERCENT_SUPPORTED |
|---|---|
| **FTE Equivalent:** | |
| **Total Number:** | |

## Names of Faculty Supported

| NAME | PERCENT_SUPPORTED | National Academy Member |
|---|---|---|
| Robert W. Heath Jr. | 0.12 | |
| Andreas Gerstlauer | 0.12 | |
| **FTE Equivalent:** | **0.24** | |
| **Total Number:** | **2** | |

## Names of Under Graduate students supported

| NAME | PERCENT_SUPPORTED |
|---|---|
| **FTE Equivalent:** | |
| **Total Number:** | |

## Student Metrics

This section only applies to graduating undergraduates supported by this agreement in this reporting period

| | |
|---|---|
| The number of undergraduates funded by this agreement who graduated during this period: ..... | 0.00 |
| The number of undergraduates funded by this agreement who graduated during this period with a degree in science, mathematics, engineering, or technology fields:..... | 0.00 |
| The number of undergraduates funded by your agreement who graduated during this period and will continue to pursue a graduate or Ph.D. degree in science, mathematics, engineering, or technology fields:..... | 0.00 |
| Number of graduating undergraduates who achieved a 3.5 GPA to 4.0 (4.0 max scale): ..... | 0.00 |
| Number of graduating undergraduates funded by a DoD funded Center of Excellence grant for Education, Research and Engineering: ..... | 0.00 |
| The number of undergraduates funded by your agreement who graduated during this period and intend to work for the Department of Defense ..... | 0.00 |
| The number of undergraduates funded by your agreement who graduated during this period and will receive scholarships or fellowships for further studies in science, mathematics, engineering or technology fields: ..... | 0.00 |

## Names of Personnel receiving masters degrees

| NAME |
| --- |
| Nachiappan Valliappan |
| Jonathan Starr |
| **Total Number:** 2 |

## Names of personnel receiving PHDs

| NAME |
| --- |
| Omar El Ayach |
| Behrang Nosrat Makouei |
| **Total Number:** 2 |

## Names of other research staff

| NAME | PERCENT_SUPPORTED |
| --- | --- |
| **FTE Equivalent:** | |
| **Total Number:** | |

## Sub Contractors (DD882)

## Inventions (DD882)

## Scientific Progress

# Technology Transfer

# High Throughput via Cross-Layer Interference Alignment for Mobile Ad Hoc Networks Summary of Scientific Progress

Robert W. Heath, Jr.*†

August 26, 2013

## Contents



*The authors is with the Department of Electrical and Computer Engineering, The University of Texas at Austin, Austin, TX 78712 USA (e-mail: rheath@ece.utexas.edu).

†This work was supported the Army Research Labs, Grant W911NF1010420.

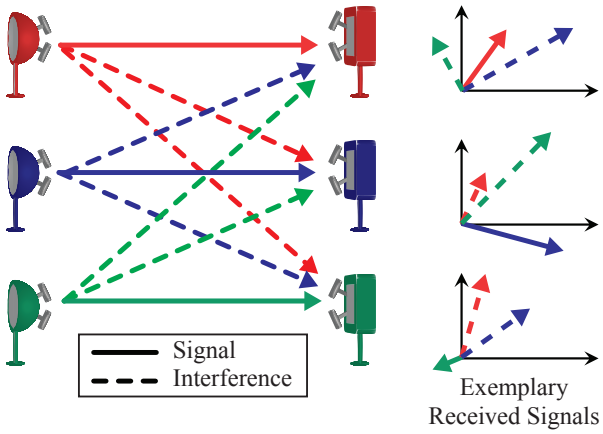


Figure 1: A 3-user interference channel.

# 1 The Studied Problem

Interference is a major impairment to successful communication in commercial and military wireless systems. In mobile ad hoc networks, interference is created when different transmitters share the same channel resource. Uncontrolled interference reduces data rates throughout the network and causes outages at dense locations. The medium access control protocol typically limits the number of simultaneous conversations and consequently the system performance. Interference is thus a critical impairment in ad hoc networks. Communication in the presence of interference is often analyzed using an abstraction known as the interference channel. In the example interference channel of Fig. 1, three different transmitters wish to communicate with three receivers. Each transmitter has a message only for its paired receiver. Assuming the transmitters share the same time and frequency resources, each transmission creates interference at the unintended receivers. There may be other sources of interference, not illustrated, such as jamming in military networks, or self-interference created from nonlinearities in the radio frequency components; those sources are not captured in the basic interference channel.

The general capacity of the interference channel and the design of practical schemes approaching the known upper bounds on sum rates have been of great interest over the last 30 years. The earliest attempts to characterize the capacity region of the interference channel, inspired by the framework established by Shannon in [1], were focused on two-user interference channels. Although the special cases of strong and very strong interference have been solved [2, 3], the general capacity of the interference channel is still an open problem. The difficulty lies in the dependence between the receivers such that the existing limiting expressions [4,5] require optimization over many variables rendering them useless for practical purposes. Recently, a series of attempts have been made to describe an approximation of the asymptotic sum capacity behavior known as the maximum achievable multiplexing gain or *degrees of freedom* (DoF) [6] where the focus is on the high SNR regime and constructing interference-free signals at the receivers. The DoF studies paved the way for a novel method of dealing with interference, known as *interference alignment* [6, 7].

Interference alignment is a linear precoding technique in which users, without directly

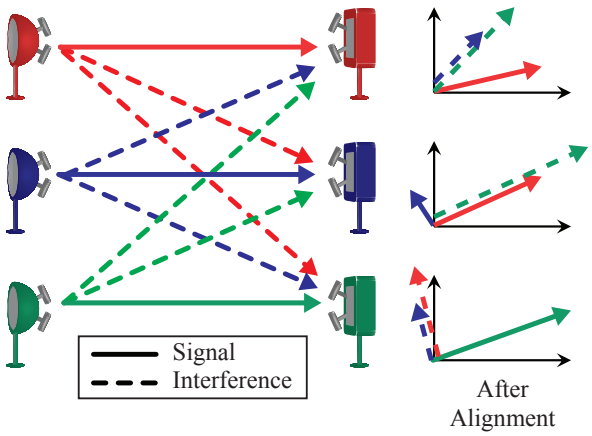


Figure 2: A 3-user $2 \times 2$ MIMO interference channel where using IA interference at each receiver is confined to a single dimension.

talking to each other, cooperatively and simultaneously transmit signals. In contrast to other interference management techniques such as orthogonal access, decoding the interference [4] or treating the interference as noise [8], interference alignment achieves the maximum multiplexing gain in a $K$-user interference channel [6] such that nodes sharing the same interference channel can achieve rates equal to one half their corresponding interference-free rates.

Consider a linear system of equations with two equations and three variables. This system can represent the received signal at two antennas where the first variable is the desired signal, the other two are the interference, and the coefficients are the channel values. In general, this underdetermined system does not have a unique solution. Assume, however, that the coefficients of the interference messages in the second equation differ from the first equation only by a scale factor. In that case, it is possible to get a single equation with the desired signal as the only variable by creating a linear combination of the two equations and solve for the desired message *interference free*. Therefore, for a general underdetermined system of equations, if there exists a relationship between coefficients of (some of) the variables, one can potentially eliminate a subset of them and if the resulting system was proper, a unique solution for some of the original variables can be found. This simple idea is the basis of interference alignment where the equations are a combination of the received signals at multiple antennas, times instances, and/or frequency tones and each receiver is only interested in a subset of the variables (the symbols transmitted by its corresponding transmitter). The mentioned dependency between the coefficients also gives a structure to the interference.

From an algebraic point of view, the goal of interference alignment is confining the aggregate interference at each receiver such that it occupies a smaller subspace than it would without any cooperation between the transmitters. Therefore, each transmitter, rather than optimizing its own link, cooperates with other transmitters to manage the interference it causes to non-intended receiver. More technically, interference alignment reduces the dimensionality of interference in the received signal space and effectively reduces the number of discernible interferers. Fig. 2 depicts the same 3-user $2 \times 2$ MIMO interference channel as in

Fig. 1 where, in this case using IA, the interference at each receiver is confined to a single dimension enabling the system to transmit 3 streams simultaneously compared to orthogonal channel access where only 2 interference-free streams can be transmitted simultaneously.

The objective of this project was to establish the viability of interference alignment in mobile ad hoc networks (MANETS) under practical assumptions. Several problems were posed and solved that provide insight into when and how interference alignment can contribute to overall performance increases in MANETS.

## 1.1 Problems Solved in Interference Alignment

This project studied several important problems in the domain of interference alignment. This section provides highlights on the most significant results. More details are provided on the solution to each problem in Section 2.

### 1.1.1 User Arrival in MIMO Interference Alignment Networks

Because of the dynamic nature of networks, it may be desirable to add a set of secondary users who desire access to the channel already being used by a set of user cooperating through interference alignment. In our work, we found the minimum number of secondary transmit antennas required so that a secondary user can use the channel without affecting the sum rate of the active users, under a zero-forcing equalization assumption. When the secondary users have enough antennas, we derived several secondary user precoders that approximately maximize the secondary users' sum rate without changing the sum rate of the active users. When the secondary users do not have enough antennas, we performed numerical optimization to find secondary user precoders that cause minimum degradation to the sum rate of the active users. Through simulations, we confirmed that i) with enough antennas at the secondary users, gains equivalent to the case of all the users cooperating through interference alignment is obtainable, and ii) when the secondary users do not have enough antennas, large rate losses at the active users can be avoided. These results have appeared in [9].

### 1.1.2 MIMO Interference Alignment in Random Access Networks

It is likely that interference alignment will not be applied simultaneously across all users in the network. Rather MANETs that employ interference alignment will support clusters of users, each performance interference alignment. In our work, we analyzed a multiple-input multiple-output (MIMO) interference channel where nodes are randomly distributed on a plane as a spatial Poisson cluster point process. Each cluster used interference alignment (IA) to suppress intra-cluster interference but unlike most work on IA, we did not neglect inter-cluster interference. We also connect the accuracy of channel state information to the distance between the nodes, i.e. the quality of CSI degrades with increasing distance. Accounting for the training and feedback overhead, we derived the transmission capacity of this MIMO IA ad hoc network and then compared it to open-loop (interference-blind) spatial multiplexing. Our simulations reveled several exemplary system setups where spatial

multiplexing outperformed IA due to the imperfect channel state information or the non-aligned inter-cluster interference. These results have been submitted for publication in [**?**]; a shorter version has already appeared in [**?**].

### 1.1.3 Interference Alignment with Distributed Antennas

Distributed antennas are one way to provide more robust transmission in wireless systems. The antennas might be distributed across several base stations, or located on different sides of a vehicle for example. Existing IA solutions cannot be applied to distributed antenna systems (DAS) as they neglect the per-remote-radio power constraints imposed on distributed precoders. This research solved the problem of how to performance IA in a distributed antenna system. Two different constraints were considered: ones with a limit on maximum per-radio power, and ones with a strict equality constraint on per-radio power. The rate-loss incurred by a simple power back-off strategy, used in systems with maximum power constraints, was characterized analytically. It was also shown that enforcing strict power constraints avoids such a rate-loss but negatively affects IA feasibility. For such systems, an IA algorithm was proposed and feasibility conditions are derived based on the concept of system properness. These results have been submitted for publication in [10].

### 1.1.4 Prototyping MIMO Interference Alignment

The performance of IA depends on the practical issues such as the performance of synchronization, channel estimation and feedback. In this paper, a prototype is implemented for the IA system with three users. There have been IA prototypes in recent years, but the previous prototypes have not considered the distribution of the nodes in IA network. The nodes are physically distributed in our prototype not sharing their time and frequency references with any other, thus working independently, which enables the experimental study of IA under the most practical setup. For the distributed system, the over-the-air schemes for time and frequency synchronization and analog feedback are studied and implemented. According to the measurement from our prototype, it is shown that IA achieves the sum rate from the previous analysis on imperfect channel information. In addition, some other measurements are performed considering the accuracy of IA solution, synchronization of nodes, and CSI feedback. For the accuracy of IA solution, the performance of IA versus the number of iterations for an iterative IA method is measured. For synchronization accuracy, the performance with different residual frequency offset is measured. Finally, for the CSI feedback quality, analog feedback and scaler quantization-based limited feedback is first compared. These results are about to be submitted for publication in [**?**]. Earlier related results were reported in [11].

# 2 Summary of the Key Results

## 2.1 User Arrival in MIMO Interference Alignment Networks

In general, a high computational complexity [12, 13] and overhead [14, 15] cost is associated with finding the IA precoders and combiners. For example, overhead is required to acquire

propagation channel state information, exchange channel state information, and to coordinate the transmissions and reception of multiple users. This overhead is incurred often, essentially every time the channel changes. Further, the amount of overhead scales super linearly with the number of users. The premise of this project is applied locally in small closed clusters to compromise between increased data rate and moderate overhead. This premise was established in prior work by the PI, where he established the optimality of performing interference alignment over small groups of users in a variety of settings including overhead and with channel estimation error.

Once a set of users have aligned their interference, it is desirable to retain their alignment status until the channels change. An example of a set of existing IA users is illustrated in Fig. 3. Most future interference-limited wireless networks, however, will be packet-switched with bursty data traffic, requiring frequent changes in the number of active users [16]. Also, the feedback overhead [17] and the number of antennas at each node [18] practically limit the number of user pairs that can cooperate through IA. Therefore, in an IA network, there will be nodes that are *arriving* to the network and, although not included in the existing IA setup, wish to communicate with their receivers. An example of new nodes joining an IA network is depicted in Fig. 3. Determining when such nodes can be admitted to the network (are allowed to transmit) and/or developing transmission strategies for them is referred to as *user arrival*. Without developing appropriate user arrival techniques for the new users, IA can not be utilized in a dynamic network without incurring overhead to reconfigure the entire network. This motivates considering the problem of user arrival in interference alignment networks.

In this work, we consider a set of active users exhausting the network resources by cooperatively utilizing IA and a further set of secondary users who wish to communicate in this network. Such a network topology can be a small part of a larger network which is, due to the limited number of antennas at each node and physical distance, clustered into separate regions. Fig. 4 depicts an ad hoc network clustered into separate IA groups and some nodes which are not part of any IA cluster. We assume the secondary users are required to have minimum impact on the performance of the active users, defined as the sum rate of the active users, and the active users ignore the presence of the secondary users when designing their precoders and/or equalizers.

The main technical contributions of this work are summarized as follows. We compute a *zero-impact* threshold for the number of secondary transmitter antennas where secondary transmitters with more (or equal) antennas than this threshold can use the communications medium without degrading the sum rate of the active users. We find optimum and suboptimum secondary user precoders for two cases: (i) when the secondary users satisfy the *zero-impact* threshold and (ii) when they do not.

When the secondary users satisfy the *zero-impact* threshold, there exists a set of precoders that will *not* degrade the sum rate of the active users. Thus, the secondary users can optimize an objective function of their own link by selecting a precoder from this set. We choose the achievable sum rate as the objective function and derive optimum and suboptimum precoders for the case of one and two secondary users respectively. For more than two secondary users, we choose the degrees of freedom (DOF) as the objective function, defined as the slope of average sum rate (b/s/Hz) versus logarithm of signal-to-noise ratio (dB) at high transmit power. We propose *successive IA* precoding and show it is optimum for various

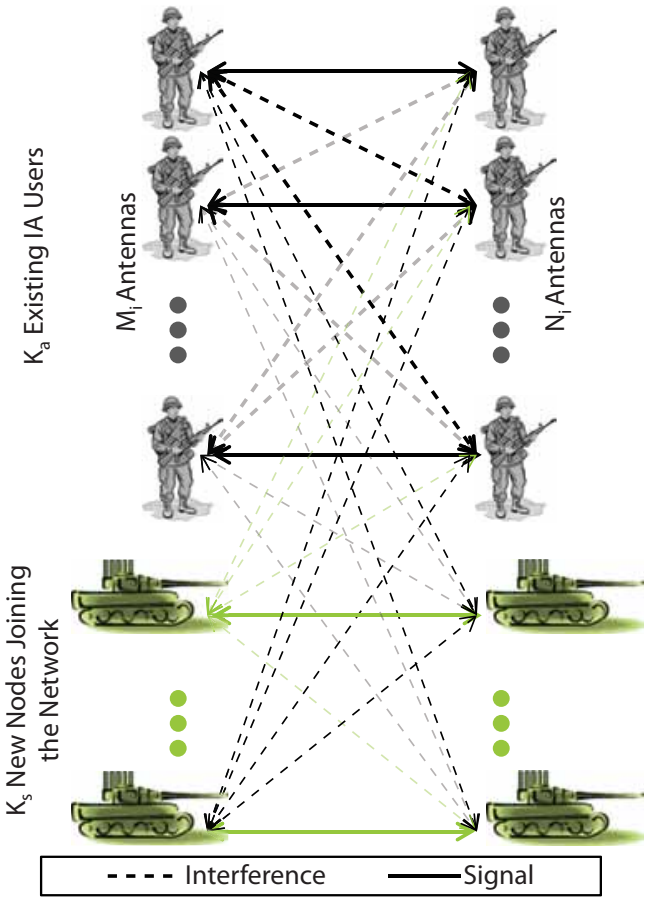


Figure 3: A set of existing IA users fully utilizing network resources and a set of new nodes joining the network.

network setups determined by the number of active users, secondary users, and antennas at each node. When the secondary users have fewer antennas than the *zero-impact* threshold, we search for secondary user precoders causing minimum degradation to the sum rate of the active users through a steepest descent search over the Grassmann manifold. For this numerical optimization, we propose three initial solutions of varying degrees of complexity.

### 2.1.1 Mathematical Framework and Problem Statement

Consider a $K_a$-user MIMO interference channel where the $i$th transmitter and receiver are equipped with $M_i$ and $N_i$ antennas, respectively. In general, each transmitter $i$ uses a precoding matrix $\mathbf{F}_i$ of dimension $M_i \times d_i$ to transmit $d_i$ streams to its corresponding receiver; which is then decoded by the $i^{th}$ receiver after processing the received signal with a combining matrix $\mathbf{W}_i$. As precoders with orthonormal columns are preferred in MIMO channels [19], we assume $\mathbf{F}_i \in \mathcal{O}$ where $\mathcal{O}$ is the set of matrices with orthonormal columns. For each time

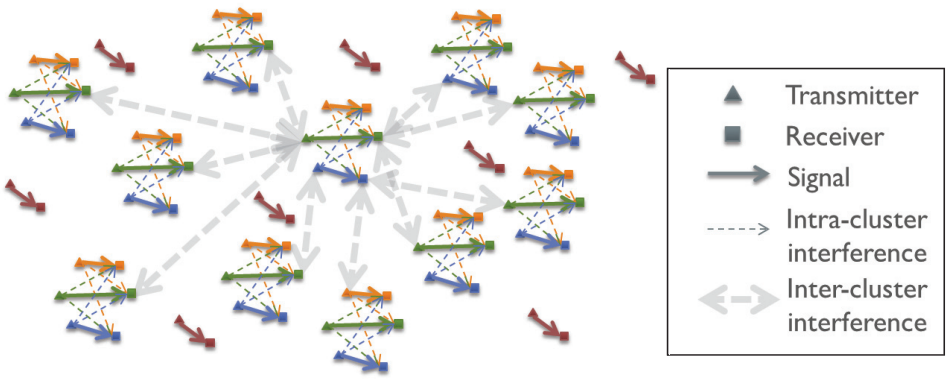


Figure 4: An ad hoc network partitioned into separate IA clusters which some transmit/receive pairs are not part of any IA clusters.

instant, the received signal at the $i$th receiver, with perfect timing and synchronization, is

$$\mathbf{y}_i = \sum_{k=1}^{K_a} \mathbf{H}_{ik}\mathbf{F}_k\mathbf{x}_k + \mathbf{z}_i \quad i = 1, \ldots, K \tag{1}$$

where $\mathbf{H}_{ik}$ is the matrix of channel coefficients of a block fading channel between transmitter $k$ and receiver $i$, the transmitted signal from the $i$th node is $\mathbf{x}_i$ with power constraint $\mathbb{E}\{\mathbf{x}_i^*\mathbf{x}_i\} = P$ and $\mathbf{z}_i$ is the AWGN with elements in $\mathcal{CN}(0, \sigma^2)$ where $\sigma^2$ is the noise power spectral density which includes thermal noise and white excess interference from unaccounted sources. Moreover, we also assume $\mathbf{H}_{ik}$ has full column rank for all $i, k$ implying enough scattering in the channel.

The goal of IA for the MIMO constant channel is to design the precoding and combining matrices such that the following conditions are satisfied

$$\begin{cases} \text{rank}\left(\mathbf{W}_\text{i}\mathbf{H}_\text{ii}\mathbf{F}_\text{i}\right) = \text{d}_\text{i} \\ \mathbf{W}_i\mathbf{H}_{ik}\mathbf{F}_k = \mathbf{0}\ \forall k \neq i \end{cases} \forall i \in \{1, \ldots, K_a\}. \tag{2}$$

We assume the system of IA in (2) is feasible [18]. Feasibility of IA implies that interference from the active transmitters at the $i$th active receiver is confined to an $N_i - d_i$ dimensional subspace; assume columns of $\mathbf{C}_i$ are a non-unique basis for this interference subspace. We further assume each active receiver uses a zero-forcing equalizer, given by $\mathbf{W}_i^{ZF} = \left[\mathbf{I}_{d_i}, \mathbf{0}\right]\left[\mathbf{H}_{ii}\mathbf{F}_i, \mathbf{C}_i\right]^{-1}$. It can be shown that the total achievable sum-rate of the active users is given by

$$R_{\text{sum}}^{\text{au}} = \sum_{i=1}^{K_a}\sum_{n=1}^{d_i} \log\left(1 + \frac{\gamma_o/d_i}{\mathbf{e}_n\left(\left(\mathbf{F}_i^*\mathbf{H}_{ii}^*\mathbf{P}_i\mathbf{H}_{ii}\mathbf{F}_i\right)^{-1}\right)\mathbf{e}_n^*}\right), \tag{3}$$

where $\mathbf{P}_i = \left(\mathbf{I}_{N_i} - \mathbf{C}_i\mathbf{C}_i^*\right)$ is the projection matrix into the nullspace of the interference subspace at the $i$th active receiver, $\gamma_o = \frac{P}{\sigma^2}$ and $\mathbf{e}_n$ is the $n$th row of $\mathbf{I}_n$.

Assume $K_s$ secondary users request sharing the network resources. Define $K = K_a + K_s$, and without loss of generality, let secondary users be the last $K_s$ users in the ordered set of

user indices $\mathcal{K} = \{1, \ldots, K_a, K_a + 1, \ldots, K\}$. We assume the first $K_a$ users do not change their precoders or receiving filters when the secondary users join the network. This has two important implications: *a*) the active transmitters do not help the transmission of the secondary users, *b*) the active receivers are not aware of the interference from the secondary users.

In the presence of the secondary users, $R_{\text{sum}}^{\text{au}}$ changes from (3) to

$$\sum_{i=1}^{K_a} \sum_{n=1}^{d_i} \log \left( 1 + \frac{\gamma_o / d_i}{\mathbf{e}_n \left( \left( \mathbf{F}_i^* \mathbf{H}_{ii}^* \mathbf{P}_i \mathbf{H}_{ii} \mathbf{F}_i \right)^{-1} + \sum_{k=K_a+1}^{K} \frac{\gamma_o}{d_k} \mathbf{W}_i \mathbf{H}_{ik} \mathbf{F}_k \mathbf{F}_k^* \mathbf{H}_{ik}^* \mathbf{W}_i^* \right) \mathbf{e}_n^*} \right), \tag{4}$$

where we have assumed that $\mathbf{H}_{ik}$ is independent of $\mathbf{H}_{nm}$ for $i \neq n$ or $k \neq m$. We divide the contribution of this work into three parts corresponding to answering the following three questions

1. How many antennas does a secondary node need, $M_s$, in order to use the network resources without degrading the active user's sumrate ((4) is equal to (3))? Equivalently

$$M_s | M_i \geq M_s \quad i > K_a \rightarrow \sum_{k=K_a+1}^{K} \frac{\gamma_o}{d_k} \mathbf{W}_i \mathbf{H}_{ik} \mathbf{F}_k \mathbf{F}_k^* \mathbf{H}_{ik}^* \mathbf{W}_i^* = \mathbf{0} \tag{5}$$

2. When the secondary nodes have enough antennas, what is their optimum precoding matrices such that in addition to not degrading the sumrate of the active users the achievable sumrate of the secondary nodes is also maximized? Equivalently, we solve

$$\begin{aligned} &\underset{\mathbf{F}_{K_a+1}, \ldots, \mathbf{F}_K \in \mathcal{O}}{\arg\max} \sum_{k=K_a+1}^{K} \log \det \left( \mathbf{I} + \frac{\gamma_o}{d_s} \mathbf{H}_{kk} \mathbf{F}_k \mathbf{F}_k^* \mathbf{H}_{kk}^* (\mathbf{I}_{N_k} + \sum_{i=1, i \neq k}^{K} \frac{\gamma_o}{d_i} \mathbf{H}_{ki} \mathbf{F}_i \mathbf{F}_i^* \mathbf{H}_{ki}^*)^{-1} \right), \\ &\text{s.t.} \quad \left[ \left( \mathbf{P}_1 \mathbf{H}_{1k} \right)^*, \ldots, \left( \mathbf{P}_{K_a} \mathbf{H}_{K_a k} \right)^* \right]^* \mathbf{F}_k = \mathbf{0} \quad k = K_a + 1, \ldots, K. \end{aligned} \tag{6}$$

3. When the secondary nodes do not have enough antennas, what is their optimum precoding matrices such that the sum-rate degradation at the active users is minimized. Equivalently, we solve

$$\underset{\mathbf{F}_{K_a+1}, \ldots, \mathbf{F}_K \in \mathcal{O}}{\text{argmax}} \sum_{i=1}^{K_a} \sum_{n=1}^{d_i} \log \left( 1 + \frac{\gamma_o / d_i}{\mathbf{e}_n \left( \mathbf{Q}_i + \frac{\gamma_o}{d_s} \mathbf{W}_i \left( \sum_{k=K_a+1}^{K} \mathbf{H}_{ik} \mathbf{F}_k \mathbf{F}_k^* \mathbf{H}_{ik}^* \right) \mathbf{W}_i^* \right) \mathbf{e}_n^*} \right), \tag{7}$$

where $\mathbf{Q}_i = \left( \mathbf{F}_i^* \mathbf{H}_{ii}^* \mathbf{P}_i \mathbf{H}_{ii} \mathbf{F}_i \right)^{-1}$.

### 2.1.2 Threshold on the Number of Secondary Transmitter's Antennas

We now present a summary of the key results obtained at this work. We first present the threshold on the minimum number of transmit antennas required at the secondary nodes such that secondary nodes can communicate without degrading the sum-rate of active nodes.

Then we present the results on two scenarios, one when the secondary transmitters have enough antennas (more than this threshold) and the other when the secondary transmitters are lacking enough number of transmit antennas. With enough antennas, the secondary transmitters can avoid causing any sum-rate degradation at the active receivers where we derive optimum secondary precoders that, in addition, maximize the achievable sum-rate of the secondary nodes. Without enough antennas, the secondary transmitters are bound to decrease the sum-rate of the active nodes and in this case we present secondary transmitter precoder matrices that minimize this sum-rate loss.

As discussed before, each active receiver uses a zero-forcing to receiver to combine its signal. The zero-forcing receiver is based on projecting the received signal into the nullspace of the interference subspace at each receiver. Therefore, if the interference from the secondary transmitters is also aligned into this interference subspace, it will be cancelled without changing the signal-to-noise-plus-interference (SINR) at the active receivers. Using this fact, in [20] we prove the following Lemma.

**Lemma 1** *The $k^{th}$ >$K_a$ transmitter can send $d_k$ streams without degrading* (3) *if*

$$M_k \geq \sum_{i=1}^{K_a} d_i + d_k \quad k \in \{K_a + 1, \ldots, K\}. \tag{8}$$

Lemma 1 states that if no sum-rate degradation at the active nodes is tolerable, the number of secondary transmit antennas need to be at least equal to the sum of the streams in the active network, $\sum_{i=1}^{K_a} d_i$, plus number of the desired streams at the secondary pair itself. Note that the only parameter from the active network is the total number of streams in that network and the obtained threshold is independent of the number of antennas at the active nodes.

### 2.1.3 Enough Antennas at the Secondary Transmitters

The exact solution of (6) is out of the scope of this work (it is equivalent to solving the sum-rate maximizing solution of the MIMO interference channel) and we focus on several special case.

### 2.1.4 Single Secondary Pair

Let the columns of $\tilde{\mathbf{V}}_k \in \mathcal{O}$ span the right nullspace of $\tilde{\mathbf{H}}_k = [(\mathbf{P}_1\mathbf{H}_{1k})^*, \ldots, (\mathbf{P}_{K_a}\mathbf{H}_{K_ak})^*]^*$. In [20] we prove that for a single secondary pair, a solution for (6), $\hat{\mathbf{F}}_{K_a+1}$, is given by Lemma 2.

**Lemma 2** *For $K_s = 1$, $\hat{\mathbf{F}}_k$ sovling* (6) *equals $\tilde{\mathbf{V}}_k\hat{\mathbf{G}}_k$ where the columns of $\hat{\mathbf{G}}_k$ are the $d_s$ most significant eigenvectors of $\tilde{\mathbf{V}}_k^*\mathbf{H}_{kk}^*(\mathbf{I}_{N_k} + \sum_{i=1, i\neq k}^{K} \frac{\gamma_o}{d_i}\mathbf{H}_{ki}\mathbf{F}_i\mathbf{F}_i^*\mathbf{H}_{ki}^*)^{-1}\mathbf{H}_{kk}\tilde{\mathbf{V}}_k$ and $k = K_a+1$.*

**Two Secondary Pairs** When $K_a \gg 1$ and $K_s = 2$, in [20] we approximately solve (6) using Corollary 1. Similar to Lemma 2, let $\mathbf{F}_k = \tilde{\mathbf{V}}_k\mathbf{G}_k$. Then we have

**Corollary 1** *When $K_a \gg 1$, (6) is approximately solved by setting the columns of $\mathbf{G}_k$ to the $d_s$ most significant eigenvectors of*

$$\tilde{\mathbf{V}}_k^* \mathbf{H}_{kk}^* \left( \mathbf{I}_{N_s} + \frac{\gamma_o}{d_a} \sum_{i=1}^{K_a} \mathbf{H}_{ki} \mathbf{F}_i \mathbf{F}_i^* \mathbf{H}_{ki}^* \right)^{-1} \mathbf{H}_{kk} \tilde{\mathbf{V}}_k.$$

Basically, in [20] we show that when $K_a \gg 1$, the interference of the other secondary transmitter at each secondary receiver becomes negligible and the problem folds back to the case of $K_s = 1$.

**More Than Two Secondary Pairs** Solving (6) for $K_s > 2$ is equivalent to solving the general sum-rate maximizing precoder of the MIMO interference channel and, to date, a closed-form solution directly solving (6) for $K_s > 2$ does not exist [21]. We provide, however, a precoder design called *successive interference alignment* [20] which maximizes the multiplexing gain of the secondary network (also called the achievable degrees-of-freedom) for a certain (and plausible) network configuration. In successive interference alignment, the secondary transmitters first align their interference at the active receivers into the corresponding interference subspaces. Then, the secondary transmitters and the secondary receiver cooperatively modify the secondary precoding matrices such that a new interference alignment network is formed within the secondary nodes. We can only, however, provide a conjecture on the optimality of successive interference alignment in certain network configurations and its performance evaluation is left for future work.

**Conjecture 1** *Consider a $3K$-user interference channel for $K \in \mathbb{Z}^+$ where the transmitter/receiver pairs are divided into $K$ groups of 3 users each, $\{G_1, G_2, \ldots, G_K\}$, such that the nodes of the $i$th group have $3i-1$ antennas. Performing successive IA on the $k$th group, $2 \leq k \leq K$, through creating effective channels between the nodes of $G_k$ based on the interference subspaces and precoders of the $\{1, \ldots, k-1\}$ groups achieves the same DoF as if all the $3K$ users had done IA together.*

### 2.1.5 Not Enough Antennas at the Secondary Transmitters

In general, (7) is a complex non-convex problem and its exact solution is out of the scope of this contribution. By assuming $K_s = 1$, we simplify (7) so that a numerical optimization technique can be utilized to search for the optimum secondary precoder. The simplified objective problem, however, is still non-convex and the better the initial solution provided to the numerical optimization problem the better the final solution of the numerical search. Next we present three initial solutions with varying degrees of complexity.

**Alternating Minimization Based Initial Solution** Let $\tilde{\mathbf{W}} = \bigoplus_{i=1}^{K_a} \bigoplus_{n=1}^{d_i} \sqrt{d_i} \mathbf{e}_n \mathbf{W}_i \mathbf{H}_{is}$, $\mathbf{S} = \bigoplus_{i=1}^{K_a} \bigoplus_{n=1}^{d_i} d_i \mathbf{e}_n \mathbf{Q}_i \mathbf{e}_n^*$, and $\tilde{d} = K_a d_a$. It is inferred from (2) that $\mathbf{S}$ is full rank and at high SINR, (7) can be written as

$$\underset{\mathbf{F}_s \in \mathcal{O}}{\operatorname{argmin}} \ \log\det \left( \mathbf{I} + \frac{\gamma_o}{d_s} (\mathbf{I}_{\tilde{d}} \otimes \mathbf{F}_s^*) \tilde{\mathbf{W}}^* \mathbf{S}^{-1} \tilde{\mathbf{W}} (\mathbf{I}_{\tilde{d}} \otimes \mathbf{F}_s) \right). \tag{9}$$

Let the eigenvalue decomposition of $\tilde{\mathbf{W}}^*\mathbf{S}^{-1}\tilde{\mathbf{W}}$ be $\mathbf{U}_{\tilde{\mathbf{W}}}\mathbf{\Sigma}_{\tilde{\mathbf{W}}}\mathbf{U}^*_{\tilde{\mathbf{W}}}$. If the rows of $\mathbf{I}_{\tilde{d}} \otimes \mathbf{F}_s^*$ were equal to a linear combination of eigenvectors corresponding to zero eigenvalues in $\mathbf{\Sigma}_{\tilde{\mathbf{W}}}$, the det in (9) would attain its minimum value of 1. Therefore, ideally

$$\mathbf{I}_{\tilde{d}} \otimes \mathbf{F}_s = \tilde{\mathbf{U}}_{\tilde{\mathbf{W}}}\mathbf{A}_s, \tag{10}$$

where the columns of $\tilde{\mathbf{U}}_{\tilde{\mathbf{W}}}$ are the columns of $\mathbf{U}_{\tilde{\mathbf{W}}}$ corresponding to zero eigenvalues of $\tilde{\mathbf{W}}^*\mathbf{S}^{-1}\tilde{\mathbf{W}}$ and $\mathbf{A}_s \in \mathcal{O}$ is an $(M_s - 1)\sum_{i=1}^{K_a} d_i \times (\sum_{i=1}^{K_a} d_i)d_s$ combining matrix.

In [20], we show that (10) does not have an exact solution and we present an iterative algorithm to approximately solve (10) in the least squares sense. Assume $\mathbf{F}_s$ in (10) is given. We seek an $\mathbf{A}_s$ minimizing $||\mathbf{I}_{\tilde{d}} \otimes \mathbf{F}_s - \tilde{\mathbf{U}}_{\tilde{\mathbf{W}}}\mathbf{A}_s||_F^2$. Equivalently

$$\hat{\mathbf{A}}_s = \underset{\mathbf{A}_s \in \mathcal{O}}{\operatorname{argmax}} \ \mathfrak{Re}\left(\operatorname{tr}\left(\mathbf{A}_s^*\tilde{\mathbf{U}}^*_{\tilde{\mathbf{W}}}(\mathbf{I}_{\tilde{d}} \otimes \mathbf{F}_s)\right)\right), \tag{11}$$

where $\mathfrak{Re}\{.\}$ select the real part of a complex value. We solve the optimization problem of (11) using the solution to the "Procrustes problem" [22]. Now consider (10) but assume that this time $\mathbf{A}_s$ is given. We seek

$$\hat{\mathbf{F}}_s = \underset{\mathbf{F}_s \in \mathcal{O}}{\operatorname{argmin}} ||\mathbf{I}_{\tilde{d}} \otimes \mathbf{F}_s - \tilde{\mathbf{U}}_{\tilde{\mathbf{W}}}\mathbf{A}_s||_F^2 = \underset{\mathbf{F}_s \in \mathcal{O}}{\operatorname{argmax}} \ \mathfrak{Re}\left(\operatorname{tr}\left((\mathbf{I}_{\tilde{d}} \otimes \mathbf{F}_s)\mathbf{A}_s^*\tilde{\mathbf{U}}^*_{\tilde{\mathbf{W}}}\right)\right). \tag{12}$$

Similar to (11), in [20] we solve (12) using the general solution to the Procrustes problem.

**Interference Leakage Minimizing Initial Solution** Compared to the alternating minimization solution, a less complex (and less accurate) initial solution can be found by revisiting the constraint on the secondary user precoders required when no sum rate degradation at the active receivers is tolerable. Instead of requiring the secondary transmitters' interference to be confined in the interference subspace of each active receiver, we minimize (in the least squares sense) the *interference leakage* caused by the secondary users by solving $\operatorname{argmin}_{\mathbf{F}_s \in \mathcal{O}} ||\tilde{\mathbf{H}}_s\mathbf{F}_s||_F^2$. A solution to this problem is given by setting the columns of $\mathbf{F}_s$ to the $d_s$ least significant right singular vectors of $\tilde{\mathbf{H}}_s$.

**DoF-Preserving Initial Solution** In both the previously presented initial solutions interference from the secondary transmitter is not confined to the interference subspaces of the active receivers. Thus, the degrees-of-freedom of the active users' network is zero. By aligning the secondary transmitter's interference at some of the active receivers, however, a non-zero degrees-of-freedom can be achieved. Thus, we seek a solution to the problem of $\operatorname{argmin}_{\mathbf{F}_s \in \mathcal{O}} ||\tilde{\mathbf{H}}_s\mathbf{F}_s||_0$. Instead of directly solving this combinatorial problem [23], we find the largest subset of active receivers such that interference from the secondary transmitter can be perfectly aligned at the active receivers and by constructing $\mathbf{F}_s$ based on this subset of active receivers a non-zero multiplexing gain is achieved at the active network. Note that this solution is optimal for $d_a = 1$.

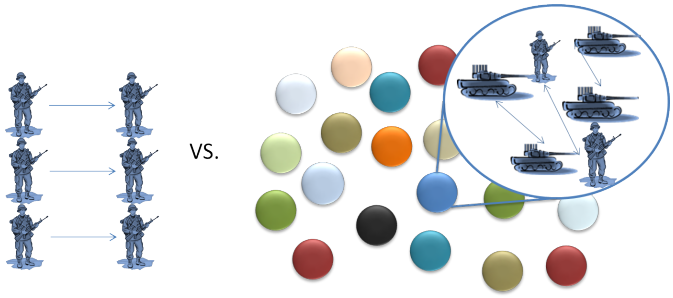


Figure 5: Traditional single cluster analysis (left) versus analyzing a large network with many such clusters in it (right).

## 2.2 MIMO Interference Alignment in Random Access Networks

In large networks, such as MANETs, IA will be used independently in separate clusters and the nearby nodes that are not coordinating with any one cluster will cause non-aligned interference at the receivers (an example of this configuration is shown Fig. 4). This is motivated by the following observations.

1. The number of antennas at each node is a limiting factor. It is shown in [24] that the number of nodes that can cooperate through MIMO IA is limited by the number of antennas at each node.

2. Overhead practically limits the cluster size. The overhead of IA grows super linearly with the number of users [25], and hence it is likely that small groups of nodes will coordinate to perform IA.

3. More cooperation is not always better. Recently, [26] showed that because of inherent channel uncertainty, there is a moderate cluster size above which spectral efficiency at best saturates, and in many practical scenarios (e.g. when pilots are used for channel estimation), actually decreases if more nodes join the cluster to cooperate.

In the context of aggregate large network performance, single cluster analysis (e.g. DoF studies) does not capture the impact of interference from the other nodes in the network and can lead to unrealistic cooperation gains which would not be attainable if the *inter-cluster* interference was accounted for [26, 27]. An example of single cluster analyzes versus analyzing a large network with many such clusters is shown in Fig. 5

Therefore, the premise of this project is that IA is applied locally in small closed groups dividing a large network into separate clusters. This premise was also established in prior work by the PI, where he established the optimality of performing interference alignment over small groups of users in a variety of settings including overhead and with channel estimation error. When dealing with large networks, a relevant metric of the system performance is the transmission capacity [28], defined as the number of successful transmission per unit area, subject to a constraint on outage probability. The transmission capacity, in contrast to other network-wide system performance metrics such as transport capacity, generally leads to closed-form expressions or tight bounds providing insight into the network design parameters [29]. Also, transmission capacity analysis generally take into account large-scale

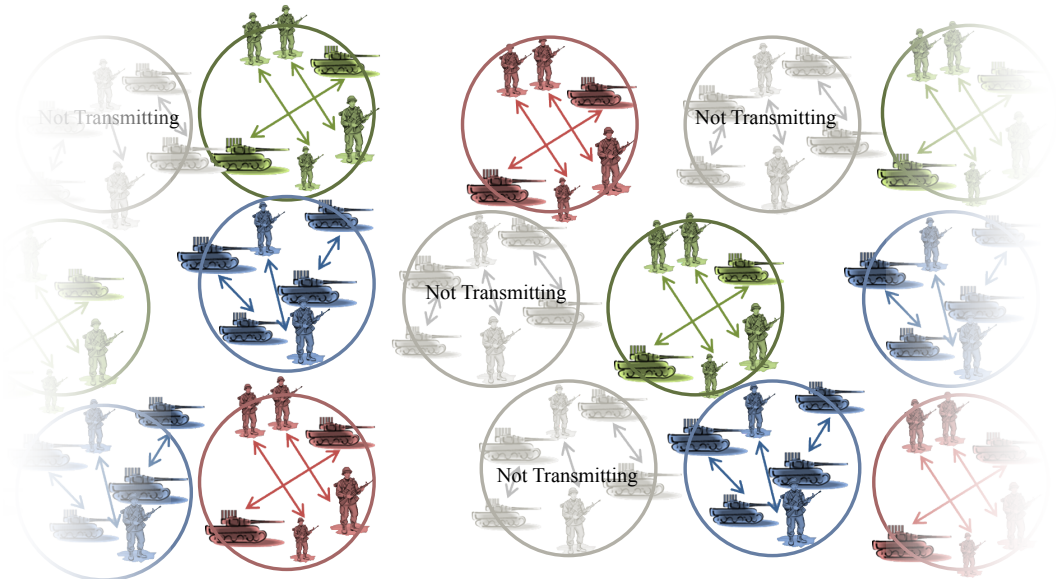


Figure 6: An Aloha-like cluster-wise channel access strategy.

fading effects, such as pathloss, which is also a key factor in determining the benefits of interference alignment in practical scenarios as for example cooperation between some nodes that are not in each other's transmission range or are not causing significant interference to their respective receivers may not be necessary and even can be counterproductive. This motivates finding the transmission capacity of decentralized networks employing cluster-wise interference alignment.

In this work, we consider a large ad hoc network where nodes are partitioned into separate clusters each cooperating through IA. We assume a four-stage transmission protocol. In the first stage, with a finite length *training period*, imperfect CSI for the cross links is obtained through MMSE channel estimation. In the second stage, the estimated CSI is fed back to the other nodes in the cluster during the *feedback period*. In the third stage, the IA transmit/receive filters are computed. In the last stage, using the rest of the finite-length channel block, the nodes communicate data using a cluster-wise slotted Aloha-like channel access protocol where at random, all nodes in a cluster either transmit simultaneously or turn off their transmission. Such a topology can represent a MANET where cooperation between close-by nodes is obtainable and the disjoint clusters can synchronize their transmission using GPS or low-overhead message passing. An example of Aloha-like cluster-wise channel access is shown in Fig. 6.

The main technical contributions of this work are summarized as follows. We first derive the point-to-point probability of outage in such a network accounting for the imperfect channel estimation. Then, we derive the optimum training period assuming a quasi-static channel maximizing cluster throughput while taking into account the feedback overhead. Finally, we derive the transmission capacity of this clustered ad hoc network and compare it with a much simpler parallel system where a single node in each cluster uses spatial multiplexing. The goal is gaining insight into the operation regimes where IA outperforms common transmission techniques by considering node density, channel block length, transmit

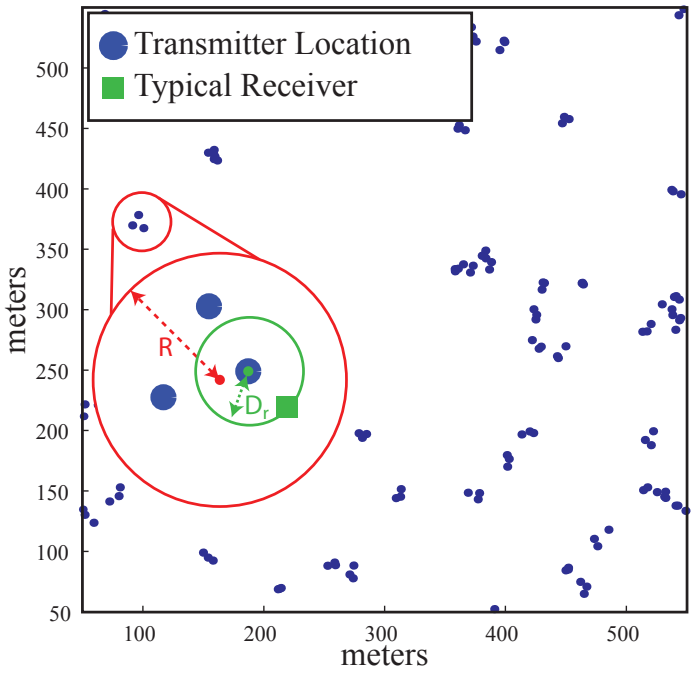


Figure 7: An instance of the transmitter's distribution when the number of transmitters per cluster is $K = 3$.

power, number of available antennas, and the number of nodes in each cluster.

### 2.2.1 Mathematical Framework and Problem Statement

The spatial locations of the potential transmitters, $\mathbf{\Phi}$, are modeled as a planar Neyman-Scott cluster point process [30]. In this process, the cluster centers are modeled by a parent homogeneous Poisson point process (PPP) $\mathbf{\Phi}_{\rm p}$ of density $\tilde{\lambda}_{\rm p}$. Each parent point $x \in \mathbf{\Phi}_{\rm p}$ forms the center of a cluster around which $K$ daughter points are uniformly distributed in a circle of radius $R$. The resulting process[1] is a stationary point process of density $K\tilde{\lambda}_{\rm p}$. We assume clusters randomly access the channel with probability $P_{\rm A}$ effectively reducing the density of this PPP to $\lambda_{\rm p} = P_{\rm A}\tilde{\lambda}_{\rm p}$. The receiver of a transmitter at $x$ is denoted by $\hat{x}$ and is assumed to be randomly located at distance $D_{\rm r}$ from its transmitter forming an $N \times N$ MIMO link. The receivers are not part of the point process $\mathbf{\Phi}$. An instance of the nodes' location is shown in Fig. 7.

In this work, a typical transmitter (a transmitter chosen at random) is considered and its performance is analyzed. This transmitter is typical in the sense that the performance of IA in this node is a representative of the average performance of IA in the network [30, 31]. Since the underlying point process is stationary, without loss of generality, it can be assumed that the typical transmitter is at the origin. Denote the cluster to which the transmitter at

[1]The parent points $\mathbf{\Phi}_{\rm p}$ will not be a part of the final point process.

the origin belongs by $\mathbf{\Psi}_o$. The received signal at receiver $\hat{x}$, $x \in \mathbf{\Psi}_o$, is

$$\mathbf{y}_{\hat{x}} = \sum_{z \in \mathbf{\Psi}_o} \sqrt{g_{\hat{x}z}} \mathbf{H}_{\hat{x}z} \mathbf{F}_z \tilde{\mathbf{s}}_z + \boldsymbol{\mathcal{I}}_{\mathrm{c}} + \mathbf{u}_{\hat{x}}, \tag{13}$$

where $\boldsymbol{\mathcal{I}}_{\mathrm{c}} = \sum_{z \in \mathbf{\Phi}/\mathbf{\Psi}_o} \sqrt{g_{\hat{x}z}} \mathbf{H}_{\hat{x}z} \mathbf{F}_z \tilde{\mathbf{s}}_z$ is the inter-cluster interference, $g_{\hat{x}z}$ and $\mathbf{H}_{\hat{x}z}$ represent the pathloss and the matrix of channel coefficients between the transmitter $z$ and the receiver $\hat{x}$, $\mathbf{F}_z$ is the precoder at transmitter $z$ with the transmitted signal $\tilde{\mathbf{s}}_z$ such that $\mathbb{E}\{\tilde{\mathbf{s}}_z^* \tilde{\mathbf{s}}_z\} = P$, and $\mathbf{u}_{\hat{x}} \sim \mathcal{CN}(\mathbf{0}, N_o \mathbf{I})$ is the additive white Gaussian noise. In this work, it is assumed that $\mathbf{F}_z^* \mathbf{F}_z = \mathbf{I}$, because of tractability and the observation that the gain attained otherwise, such as with the MMSE algorithm in [32] or the Max-SINR algorithm in [12], is limited and confined to the low SNR regime where the inter-cluster interference is generally not dominant. In every cluster, channel state information is estimated at the receivers as in [33] and conveyed to all other nodes of the cluster using an error-free instantaneous feedback link. We propose to model the uncertainty in the MIMO channels using a Gauss-Markov model of the form [34, 35]

$$\mathbf{H}_{\hat{x}z} = \sqrt{1 - \beta_{\hat{x}z}^2} \mathbf{H}_{\hat{x}z}^w + \beta_{\hat{x}z} \mathbf{E}_{\hat{x}z} \quad x, z \in \mathbf{\Psi}_o, \tag{14}$$

where $\mathbf{H}_{\hat{x}z}^w$ is the estimated channel, $\mathbf{E}_{\hat{x}z}$ represents the estimation error with i.i.d. terms distributed as $\mathcal{CN}(0,1)$, and $\beta_{\hat{x}z}^2$ is the normalized variance of the estimation error. It is assumed that the channel is quasi-static block-fading such that $\mathbf{H}$ is constant for a block duration of length $T$ and then changes independently. Training, feedback, and data transmission are assumed to be all orthogonal in time, in the same coherence time or frame $T$ [36]. Hence, $\beta_{\hat{x}z}$ is set to be related to the average received SNR at each link, $\gamma_{\hat{x}z}$, as [33, Section II.B]

$$\beta_{\hat{x}z}^2 = \frac{1}{1 + \frac{T_{\mathrm{t}}}{N} \gamma_{\hat{x}z}} = \frac{1}{1 + T_{\mathrm{t}} \frac{\gamma_{\mathrm{o}} g_{\hat{x}z}}{N}}, \tag{15}$$

where $\gamma_{\mathrm{o}} = \frac{P}{N_{\mathrm{o}}}$ and $T_{\mathrm{t}} \geq KN$ is the number of channel instances spent for training $\mathbf{H}_{\hat{x}z}$ [37]. For analytical tractability, it is also assumed that $\mathbf{H}^w$ is used to construct the precoders/equalizers and nodes effectively ignore the imperfection in CSI in their design.

At each cluster, a $K$-user system of IA is feasible if there exists a set of matrices $\mathcal{W} = \{\mathbf{W}_{\hat{z}} | z \in \mathbf{\Psi}_0\}$ such that, given the received signal of (13), the following constraints are met [6]:

$$\begin{cases} \operatorname{rank}\left(\mathbf{W}_{\hat{x}} \mathbf{H}_{\hat{x}x} \mathbf{F}_x\right) = N_s \\ \mathbf{W}_{\hat{x}} \mathbf{H}_{\hat{x}z} \mathbf{F}_z = \mathbf{0} \ \forall z \neq x \end{cases} \forall x, z \in \mathbf{\Psi}_o, \tag{16}$$

where $\mathbf{W}_{\hat{x}}$ is the combining filter used at receiver $\hat{x}$ and $N_s$ is the number of interference-free streams each transmitter can send to its receiver. The linear equalizer presented in [38] is an examples of a possible receive filter in (16). It is assumed that the IA precoders are designed using the alternating minimization algorithm in [32, Section III.A] such that $\mathbf{F}_x$ is independent of $\mathbf{H}_{\hat{x}x}$ for all $x \in \mathbf{\Psi}$. Also, it is assumed that the set of $\{N, N_s, K\}$ constitutes a feasible IA system, which for the MIMO interference channel requires that $2N - (K+1)N_s \geq 0$.

From (16), interference at receiver $\hat{x}$ is confined to an $N - N_s$ dimensional subspace. Let $[\{\cdot\}]$ represent horizontal concatenation of the elements in $\{\cdot\}$. Then, as IA precoders/equalizers are constructed using $\mathbf{H}^w$ as given by (14), the $N \times (K-1)N_s$ matrix of $\mathbf{J}_{\hat{x}} = [\{\mathbf{H}^w_{\hat{x}z}\mathbf{F}_z | z \neq x, z \in \mathbf{\Psi}_o\}]$ spans an $N - N_s$ dimensional subspace. Let the singular value decomposition of $\mathbf{J}_{\hat{x}}$ be $\mathbf{U}_{\mathbf{J}_{\hat{x}}}\mathbf{\Sigma}_{\mathbf{J}_{\hat{x}}}\mathbf{V}^*_{\mathbf{J}_{\hat{x}}}$ and let the rows of $\mathbf{W}_{\hat{x}}$ be the columns of $\mathbf{U}_{\mathbf{J}_{\hat{x}}}$ corresponding to zero singular values in $\mathbf{\Sigma}_{\mathbf{J}_{\hat{x}}}$. As $\mathbf{W}_{\hat{x}}$ is independent of $\mathbf{H}^w_{\hat{x}x}\mathbf{F}_x$, it satisfies the conditions in (16) and is a valid zero-forcing (ZF) equalizer for IA. Using this ZF receiver, the post-processing SINR of the $n$th stream at receiver $\hat{x}$ is

$$\gamma^{\mathrm{IA}}_{\hat{x},n} = \frac{g_{\hat{x}x}(1-\beta^2_{\hat{x}x})\tilde{\mathbf{h}}^*_{\hat{x}x}\tilde{\mathbf{h}}_{\hat{x}x}}{\frac{N_s}{\gamma_o} + \underbrace{g_{\hat{x}x}\beta^2_{\hat{x}x}\tilde{\mathbf{e}}^*_{\hat{x}x}\tilde{\mathbf{e}}_{\hat{x}x}}_{I_s} + \underbrace{\sum_{z\in\mathbf{\Psi}_o/x} g_{\hat{x}z}\beta^2_{\hat{x}z}\tilde{\mathbf{e}}^*_{\hat{x}z}\tilde{\mathbf{e}}_{\hat{x}z}}_{I_e} + \underbrace{\sum_{z\in\mathbf{\Phi}/\mathbf{\Psi}_o} g_{\hat{x}z}\tilde{\mathbf{h}}^*_{\hat{x}z}\tilde{\mathbf{h}}_{\hat{x}z}}_{I_i}}, \tag{17}$$

where for all $z \in \mathbf{\Phi}$, $\tilde{\mathbf{h}}_{\hat{x}z} = (\mathbf{e}^*_n\mathbf{W}_{\hat{x}}\mathbf{H}^w_{\hat{x}z}\mathbf{F}_z)^*$, $\tilde{\mathbf{e}}_{\hat{x}z} = (\mathbf{e}^*_n\mathbf{W}_{\hat{x}}\mathbf{E}_{\hat{x}z}\mathbf{F}_z)^*$, and $\mathbf{e}_n$ is the $n$th column of an $N_s \times N_s$ identity matrix. Note that $I_s$ represents the residual error from the direct link and, as the distance between the transmitter and receiver is constant, its pathloss (and the error variance) are not random variables and so it is separated from $I_e$ to emphasize this point. Let the entries of $\mathbf{H}_{\hat{x}z}$ and $\mathbf{E}_{\hat{x}z}$ be i.i.d. Gaussian terms. As $\mathbf{W}_{\hat{x}}$ and $\mathbf{F}_z$ are unitary matrices independent of $\mathbf{H}_{\hat{x}z}$ and $\mathbf{E}_{\hat{x}z}$, due to the doubly unitarily invariance of the Gaussian distribution, $\tilde{\mathbf{h}}_{\hat{x}z}$ and $\tilde{\mathbf{e}}_{\hat{x}z}$ will be column vectors of length $N_s$ with i.i.d. Gaussian terms and independent of each other (as $\mathbf{H}_{\hat{x}z}$ and $\mathbf{E}_{\hat{x}z}$ are independent of each other). Note that (17) is in fact independent of the stream index $n$. We divide the contribution of this work into three parts corresponding to answering the following three questions

1. Given the SINR expression in (17), what is the point-to-point probability of outage? Equivalently, given the SINR threshold of $\theta$, we seek to find

$$\mathrm{P}^{\mathrm{IA}}_{\mathrm{s}}(\theta) = \mathbb{P}^{!o}(\gamma^{\mathrm{IA}}_{\hat{o},n} > \theta),$$

   where $\hat{o}$ is the receiver corresponding to a *typical* transmitter located at the origin. If point-to-point outage is of interest, this analysis reveals the dependency of performance on important system parameters such as training period length, transmit power, number of antennas, density of the nodes, and pathloss.

2. For a given block fading of length $T$, what is the optimum training length $\hat{T}_{\mathrm{t}}$ locally maximizing the goodput of each cluster? Equivalently, we solve

$$\hat{T}_{\mathrm{t}} = \arg\max_{T_{\mathrm{t}}} \quad \frac{T - K^2N - T_{\mathrm{t}}}{T} KN_s\mathrm{P}^{\mathrm{IA}}_{\mathrm{s}}(\theta)\log_2(1+\theta)$$
$$\text{s.t.} \quad KN \leq T_{\mathrm{t}} \leq T - K^2N$$

   Finding the optimum training period gives insight into the overhead associated with IA compared to the other well known transmission techniques.

3. Let $q(\lambda_p) = 1 - \mathrm{P}_{\mathrm{s}}^{\mathrm{IA}}(\theta) = \epsilon$ be the maximum cluster density corresponding to the outage threshold of $\theta$. Accounting for overhead, we seek the normalized transmission capacity defined is

$$C(\epsilon) = \frac{T - K^2 N - \hat{T}_{\mathrm{t}}}{T} q^{-1}(\epsilon) K(1-\epsilon).$$

The transmission capacity hints at maximum spectral efficiency attainable by MIMO IA in a decentralized network.

### 2.2.2 Point-to-Point Outage Probability

Now we present a summary of the key results obtained at this work. In this section we derive the exact point-to-point outage probability at a typical receiver. Then, assuming fixed feedback overhead, we solve for the optimum training period locally maximizing each cluster's goodput. Next, we derive the exact transmission capacity for the case of a single data stream from each transmitter. Finally, we present an upper bound on the transmission capacity for the case of arbitrary number of streams from each transmitter. Detailed results are presented in [39–41, Chapter 3].

In (17), since $\tilde{\mathbf{h}}_{\hat{x}z}^{*}\tilde{\mathbf{h}}_{\hat{x}z}$ and $\tilde{\mathbf{e}}_{\hat{x}z}^{*}\tilde{\mathbf{e}}_{\hat{x}z}$ are i.i.d. $\Gamma(N_s, 1)$ random variables, we denote them both by $h_{\hat{x}z}$ for notational simplicity. Denote the typical transmitter at the origin by $o$. Considering a transmitter at the origin is equivalent to conditioning on the existence of a point at the origin. Since every point belongs to some cluster, conditioning on the existence of a point at the origin equals the presence of a cluster with a daughter point at the origin. Since the parent point process is a PPP, an additional cluster with a daughter point at the origin can be added to it without changing the statistics of the other points of the process. Succinctly, the Palm probability of a Newman-Scott cluster process is $\mathbb{P}^o = \mathbb{P} * \mathbf{\Psi}_o$ where $*$ denotes superposition [30]. This implies that assuming a point of the cluster process at the origin equals the original point process $\mathbf{\Phi}$ plus an additional cluster which has a point at the origin. Also this additional cluster at the origin $\mathbf{\Psi}_o$ is independent of the original process $\mathbf{\Phi}$. Since the tagged transmitter at origin does not contribute to the interference at the receiver, it is convenient to use the reduced Palm probability denoted by $\mathbb{P}^{!o}$ instead of Palm probability. Reduced Palm probability is similar to Palm probability, except that the point at the origin is not considered in the computation of the probability and hence $\mathbb{P}^{!o} = \mathbb{P} * \{\mathbf{\Psi}_o \setminus \{o\}\}$. From (17), the probability of success is therefore $\mathrm{P}_{\mathrm{s}}^{\mathrm{IA}}(\theta) = \mathbb{P}^{!o}(\gamma_{\hat{o},n}^{\mathrm{IA}} > \theta)$, where $\theta$ is the SINR threshold.

**Theorem 1** *For the system model described in Section 2.2.1, the success probability when each cluster uses IA is*

$$\mathrm{P}_{\mathrm{s}}^{\mathrm{IA}}(\theta) = \sum_{k=0}^{N_s-1} \frac{(-\eta)^k}{k!} \frac{\mathrm{d}^k}{\mathrm{d}s^k} e^{-s\frac{N_{\mathrm{s}}}{\gamma_{\mathrm{o}}}} \left( \frac{\frac{T_{\mathrm{t}}\gamma_{\mathrm{o}}}{N} + D_{\mathrm{r}}^{\alpha}}{s + \frac{T_{\mathrm{t}}\gamma_{\mathrm{o}}}{N} + D_{\mathrm{r}}^{\alpha}} \right)^{N_s} \mathcal{L}_{\mathtt{I}_e}^{!o}(s) \mathcal{L}_{\mathtt{I}_i}(s) \Big|_{s=\eta}, \tag{18}$$

*where $\mathcal{L}_{\mathtt{I}_e}^{!o}(s)$ and $\mathcal{L}_{\mathtt{I}_i}(s)$ are Laplace transforms of intra and inter-cluster interference given*

*by*

$$\mathcal{L}^{!o}_{\mathtt{I}_e}(s) = \frac{1}{\pi R^2} \int\limits_{B(o,R)} \left[ \frac{1}{\pi R^2} \int\limits_{B(o,R)} \left( \frac{\frac{T_\mathrm{t}\gamma_\mathrm{o}}{N} + \|x-y-\hat{o}\|^\alpha}{s + \frac{T_\mathrm{t}\gamma_\mathrm{o}}{N} + \|x-y-\hat{o}\|^\alpha} \right)^{N_s} \mathrm{d}x \right]^{K-1} \mathrm{d}y, \tag{19}$$

$$\mathcal{L}_{\mathtt{I}_i}(s) = \exp\left( -\lambda_p \int\limits_{\mathbb{R}^2} 1 - \left[ \frac{1}{\pi R^2} \int\limits_{B(o,R)} \left( \frac{\|x-y\|^\alpha}{s+\|x-y\|^\alpha} \right)^{N_s} \mathrm{d}x \right]^K \mathrm{d}y \right), \tag{20}$$

*where* $\eta = \frac{\theta}{g_{\hat{o}o}(1-\beta^2_{\hat{o}o})}$.

### 2.2.3 Optimum Training Period

For a given block fading of length $T$, the transmitters spend $T_\mathrm{t} \geq KN$ channel instances for training the links. We also assume a prefect analog feedback link where the receivers send the trained channels over a period of $T_\mathrm{f} = K^2N$ channel instances to the transmitters. In practice, the transmitters select $T_\mathrm{t}$ to optimize some performance criteria. In this work, we assume transmitters use the goodput at each cluster defined as

$$\begin{aligned} \hat{T}_\mathrm{t} = \arg\max_{T_\mathrm{t}} \quad & \frac{T - K^2N - T_\mathrm{t}}{T} KN_s \mathrm{P}_\mathrm{s}^{\mathrm{IA}}(\theta) \log_2(1+\theta) \\ \text{s.t.} \quad & KN \leq T_\mathrm{t} \leq T - K^2N, \end{aligned} \tag{21}$$

where $\frac{T-K^2N-T_\mathrm{t}}{T}$ accounts for the transmission opportunities lost due to overhead, $KN_s$ is the total number of streams in each cluster, and $\mathrm{P}_\mathrm{s}^{\mathrm{IA}}(\theta)\log_2(1+\theta)$ is the rate multiplied by the times the *connection exists*, i.e. SINR passes the threshold $\theta$. Note that in (21), $\mathrm{P}_\mathrm{s}^{\mathrm{IA}}(\theta)$ is implicitly a function of the training period $T_\mathrm{t}$.

For a given node mobility and hence a Doppler frequency $f_d \approx \frac{1}{T}$, the training period can be written as a fraction of the total block length $T$, i.e. $T_\mathrm{t} = \delta T = \delta \frac{1}{f_d}$. Therefore, the optimization problem of (21) can be rewritten as

$$\begin{aligned} \hat{\delta} = \arg\max_{\delta} \quad & (1 - \delta - f_d K^2 N) KN_s \mathrm{P}_\mathrm{s}^{\mathrm{IA}}(\theta) \log_2(1+\theta) \\ \text{s.t.} \quad & f_d KN \leq \delta \leq (1 - f_d K^2 N), \end{aligned} \tag{22}$$

where

$$\mathrm{P}_\mathrm{s}^{\mathrm{IA}} = \sum_{k=0}^{N_s-1} \frac{(-\eta)^k}{k!} \frac{\mathrm{d}^k}{\mathrm{d}s^k} e^{-s\frac{N_s}{\gamma_\mathrm{o}}} \left( \frac{\frac{\delta\gamma_\mathrm{o}}{N} + f_d D_r^\alpha}{\frac{\delta\gamma_\mathrm{o}}{N} + f_d(s + D_\mathrm{r}^\alpha)} \right)^{N_s} \mathcal{L}^{!o}_{\mathtt{I}_e}(s, f_d) \mathcal{L}_{\mathtt{I}_i}(s) \Big|_{s=\eta},$$

$\eta = \frac{\theta {D_r}^\alpha (\gamma_\mathrm{o}\delta + N {D_r}^\alpha f_d)}{\gamma_\mathrm{o}\delta}$, $\mathcal{L}^{!o}_{\mathtt{I}_e}(s, f_d) = \frac{1}{\pi R^2} \int\limits_{B(o,R)} \left[ \frac{1}{\pi R^2} \int\limits_{B(o,R)} \frac{\frac{\delta\gamma_\mathrm{o}}{N} + f_d\|x-y-\hat{o}\|^\alpha}{\frac{\delta\gamma_\mathrm{o}}{N} + f_d(s+\|x-y-\hat{o}\|^\alpha)} \mathrm{d}x \right]^{K-1} \mathrm{d}y$ , and $\mathcal{L}_{\mathtt{I}_i}(s)$ is given by (20).

With a convex relaxation on $T_\mathrm{t}$ (and therefore $\delta$) to change its domain to the real numbers, the optimization problem of (22) is convex and solvable with any of the numerical optimization algorithms [42]. Note that, although complicated, the derivative of the objective

function in (22) w.r.t $\delta$ is computable and evaluating the objective function or its derivatives for any set of values is possible. Next we provide approximate closed form solutions for some common cases.

When $N_s = 1$, $\mathrm{P_s^{IA}}$ in (22) simplifies to

$$\mathrm{P_s^{IA}}(N_s = 1) = e^{-\eta \frac{N_s}{\gamma_o}} \frac{\frac{\delta\gamma_o}{N} + f_d D_r^{\alpha}}{\frac{\delta\gamma_o}{N} + f_d(\eta + D_r^{\alpha})} \mathcal{L}_{\mathtt{I}_e}^{!o}(\eta, f_d)\mathcal{L}_{\mathtt{I}_i}(\eta). \tag{23}$$

The highly non-linear dependency of (23) on $\delta$ can be converted into a polynomial one following the Taylor expansion approximation method proposed in [43]. Let $g(\delta, f_d)$ be the objective function in (22). Rewrite $g(\delta, f_d)$ as its Taylor series around $f_d = 0$ (infinite block length and hence perfect training) keeping all the other variables constant

$$\begin{aligned} \hat{\delta} \approx \arg\max_{\delta} \quad & g(\delta, f_d = 0) + \frac{\partial g}{\partial f_d}|_{f_d=0} f_d + \frac{1}{2}\frac{\partial^2 g}{\partial f_d^2}|_{f_d=0} f_d^2 \\ \text{s.t.} \quad & f_d KN \leq \delta \leq (1 - f_d K^2 N). \end{aligned} \tag{24}$$

Simplifying the terms in (24) and removing the constant scaling coefficients from the optimization problem yields

$$\begin{aligned} \hat{\delta}_1 \approx \operatorname*{argmax}_{\delta} \quad & -\delta + C_1 \frac{1}{\delta} + C_2 \frac{1}{\delta^2} \\ \text{s.t.} \quad & f_d KN \leq \delta \leq (1 - f_d K^2 N), \end{aligned} \tag{25}$$

where $C_1$ and $C_2$ are given in Appendix [40, Appendix D]. Let $\delta_1$ be the relevant root of the first derivative of (25). The optimum training period will be given by

$$\hat{T}_{t,1} = \min\left(\max\left(KN, [\delta_1 T]\right), T - K^2 N\right). \tag{26}$$

### 2.2.4 Transmission Capacity

Let $q(\lambda_p) = 1 - \mathrm{P_s^{IA}}(\theta) = \epsilon$. Accounting for overhead, the normalized transmission capacity is

$$C(\epsilon) = \frac{T - K^2 N - \hat{T}_{\mathrm{t}}}{T} q^{-1}(\epsilon) K(1 - \epsilon). \tag{27}$$

With the probability of successful transmission as given by (18), the exact expression of $q^{-1}(\epsilon)$ for general $N_s$ is not analytically tractable. Next we give its exact expression for the case of $N_s = 1$ and provide a bound for general $N_s > 1$.

**Single stream from each transmitter** Using (18)

$$q(\lambda_p) = 1 - e^{-\hat{\eta}\frac{N_s}{\gamma_o}} \left( \frac{\frac{\hat{T}_{\mathrm{t}}\gamma_o}{N} + D_{\mathrm{r}}^{\alpha}}{s + \frac{\hat{T}_{\mathrm{t}}\gamma_o}{N} + D_{\mathrm{r}}^{\alpha}} \right) \mathcal{L}_{\mathtt{I}_e}^{!o}(\hat{\eta})\mathcal{L}_{\mathtt{I}_i}(\hat{\eta}) = \epsilon, \tag{28}$$

where $\hat{\eta} = \eta|_{T_{\mathrm{t}}=\hat{T}_{\mathrm{t}}}$. Substituting (19) and (20) into (28) gives

$$q^{-1}(\epsilon) = \lambda_p^{\epsilon} = \frac{\log_e\left(\frac{e^{-\hat{\eta}\frac{N_s}{\gamma_{\mathrm{o}}}}}{1-\epsilon}\frac{\frac{\hat{T}_{\mathrm{t}}\gamma_{\mathrm{o}}}{N}+D_{\mathrm{r}}^{\alpha}}{\frac{\hat{T}_{\mathrm{t}}\gamma_{\mathrm{o}}}{N}+\hat{\eta}+D_{\mathrm{r}}^{\alpha}}\frac{1}{\pi R^2}\int\limits_{B(o,R)}\left[\frac{1}{\pi R^2}\int\limits_{B(o,R)}\left(\frac{\frac{\hat{T}_{\mathrm{t}}\gamma_{\mathrm{o}}}{N}+\|x-y-\hat{o}\|^{\alpha}}{\hat{\eta}+\frac{\hat{T}_{\mathrm{t}}\gamma_{\mathrm{o}}}{N}+\|x-y-\hat{o}\|^{\alpha}}\right)^{N_s}\mathrm{d}x\right]^{K-1}\mathrm{d}y.\right)}{\int\limits_{\mathbb{R}^2}1-\left[\frac{1}{\pi R^2}\int\limits_{B(o,R)}\left(\frac{\|x-y\|^{\alpha}}{\hat{\eta}+\|x-y\|^{\alpha}}\right)^{N_s}\mathrm{d}x\right]^{K}\mathrm{d}y}, \tag{29}$$

where $\hat{T}_{\mathrm{t}}$ is the optimum training period obtained earlier. Using (29), (27) can be computed.

**Greater than one stream from each transmitter** When $\hat{\eta} > (N_s - 1)/e$, using [40, Lemma 2]

$$q(\lambda_p) \geq 1 - \sum_{k=0}^{N_s-1}\frac{\hat{\eta}^k}{k!}e^{-(\hat{\eta}-k/e)\frac{N_s}{\gamma_{\mathrm{o}}}}\mathbb{E}e^{-(\hat{\eta}-k/e)g_{\hat{o}o}\beta_{\hat{o}o}^2 h_{\hat{o}o}}\mathcal{L}_{\mathtt{I}_e}^{!o}(\hat{\eta}-k/e)\mathcal{L}_{\mathtt{I}_i}(\hat{\eta}-k/e). \tag{30}$$

Now, if $\hat{\eta} \gg k/e$ for all $k \in \{0, \ldots, N_s - 1\}$, $\hat{\eta} - k/e \approx \hat{\eta}$ and hence (30) equals

$$\begin{aligned} q(\lambda_p) &\geq 1 - \left(\sum_{k=0}^{N_s-1}\frac{\hat{\eta}^k}{k!}\right)e^{-\hat{\eta}\frac{N_s}{\gamma_{\mathrm{o}}}}\mathbb{E}e^{-\hat{\eta}g_{\hat{o}o}\beta_{\hat{o}o}^2 h_{\hat{o}o}}\mathcal{L}_{\mathtt{I}_e}^{!o}(\hat{\eta})\mathcal{L}_{\mathtt{I}_i}(\hat{\eta}) \\ \Rightarrow \mathcal{L}_{\mathtt{I}_i}(\hat{\eta}) &\geq \frac{1-\epsilon}{\left(\sum_{k=0}^{N_s-1}\frac{\hat{\eta}^k}{k!}\right)e^{-\hat{\eta}\frac{N_s}{\gamma_{\mathrm{o}}}}\mathbb{E}e^{-\hat{\eta}g_{\hat{o}o}\beta_{\hat{o}o}^2 h_{\hat{o}o}}\mathcal{L}_{\mathtt{I}_e}^{!o}(\hat{\eta})} \\ \Rightarrow \lambda_p^{\epsilon} &\leq \frac{\log_e\left(\frac{1}{1-\epsilon}\left(\sum_{k=0}^{N_s-1}\frac{\hat{\eta}^k}{k!}\right)e^{-\hat{\eta}\frac{N_s}{\gamma_{\mathrm{o}}}}\mathbb{E}e^{-\hat{\eta}g_{\hat{o}o}\beta_{\hat{o}o}^2 h_{\hat{o}o}}\mathcal{L}_{\mathtt{I}_e}^{!o}(\hat{\eta})\right)}{\int\limits_{\mathbb{R}^2}1-\left[\frac{1}{\pi R^2}\int\limits_{B(o,R)}\left(\frac{\|x-y\|^{\alpha}}{\hat{\eta}+\|x-y\|^{\alpha}}\right)^{N_s}\mathrm{d}x\right]^{K}\mathrm{d}y}. \end{aligned} \tag{31}$$

### 2.2.5 Intuition Obtained from the Results

Our results indicate that selecting IA as the transmission technique of choice in a MANET should be based on the node density, the mobility of the nodes, the transmit power, and the characteristics of the underlying communications medium. For example, in dense networks with high transmit power, spatial multiplexing (SM) over an orthogonal channel access strategy such as time division multiple access (TDMA) can outperform IA due to lower inter-cluster interference. Also, the signal-to-noise-ratio (SNR) switching point between IA and TDMA+SM decreases with increasing density and mobility. In conclusion, MIMO IA is best suited for low Doppler disperse clusters of nodes capable of local coordination.

## 2.3 Interference Alignment with Distributed Antennas

Interference alignment is a transmission strategy that is designed to maximize the number of non-interfering symbols that can be simultaneously communicated over an interference network [6]. By doing so, IA achieves the maximum degrees of freedom in a variety of

single or multi-antenna interference channels and consequently allows systems to approach capacity in the high signal-to-noise ratio (SNR) regime. In the more practically relevant regime of low-to-medium SNR, however, IA's sum-rate performance has been shown to be suboptimal [44–48]. This limits the applicability of IA in practical network with reasonable transmit power budgets since it does little to improve the rates for the disadvantaged low-SNR users [49]. To overcome this practical shortcoming, prior work has focused on the development of enhanced precoding strategies that improve on IA's low-SNR performance. The unifying concept behind the algorithms in [47, 48, 50, 51] is to potentially forgo perfect alignment and optimize objective functions that are more tightly related to system sum-rate. In addition to better algorithms, however, IA's utility can be improved by considering network architectures that may be more suitable for such a high-SNR transmission strategy. One such network is systems with distributed antennas. In fact, the merits of combining distributed antennas with cooperative, or multi-user transmission strategies, have previously been established by the PI in the case of the multi-user MIMO broadcast channel [52, 53].

In this work we consider the application of interference alignment to networks with distributed antenna transmitters. The motivation for combining IA with DAS is two-fold. First, DAS may help overcome or avoid IA's low-SNR weakness by boosting signal power for distant users. Second, IA may constitute an effective co-channel interference management strategy for DAS. Since existing IA solutions neglect per-RRU (or per-antenna) power constraints, and are thus not applicable to DAS, we focus on reevaluating the possibility and performance of IA in these more tightly constrained systems. We note that while the antenna's geographic separation in DAS necessitates the consideration of such power constraints, per-antenna constraints are in fact of practical relevance in all wireless transceivers that must operate with power-efficiency in mind, i.e., even those with co-located antennas [54–58].

We consider IA in two types of DAS, ones in which individual RRU powers are upper bounded (called *maximum power constraints*) and others in which all RRUs must transmit at a constant power level (called *strict power constraints*) [56]. This work thus completes the preliminary results presented in [59] which focused on the special case of IA with per-antenna power constraints in co-located antenna systems. To satisfy maximum power constraints, we consider a simple strategy of transmit power back-off and show that the back-off procedure incurs a systematic loss in sum-rate. To gain a better quantitative understanding of the sum-rate loss due to back-off, we give an analytical characterization of the back-off factor's statistics under the simplifying assumption of channels with equal pathloss, i.e., in the case of co-located antennas. The development of more sophisticated IA strategies that satisfy maximum power constraints and avoid the loss incurred by back-off is an interesting topic for future work. In systems where RRUs must transmit at a fixed power level, we show that the addition of such strict power constraints negatively affects the feasibility of IA. In other words, realizing IA with strict power constraints requires more antennas at the transmitters or receivers. To examine this reduction in feasibility, we leverage the methodology in [60] to derive properness conditions for IA systems with strict per-RRU power constraints. While properness and feasibility are in general not equivalent, the results of [61–63] indicate that proper systems are most often feasible except in a few corner cases. As a result, properness can provide a simple and sufficiently accurate predictor of IA feasibility. To further demonstrate the true feasibility of IA in proper systems, we present a simple iterative IA algorithm based on the alternating minimization solution in [51, 64]. While more sophisticated algo-

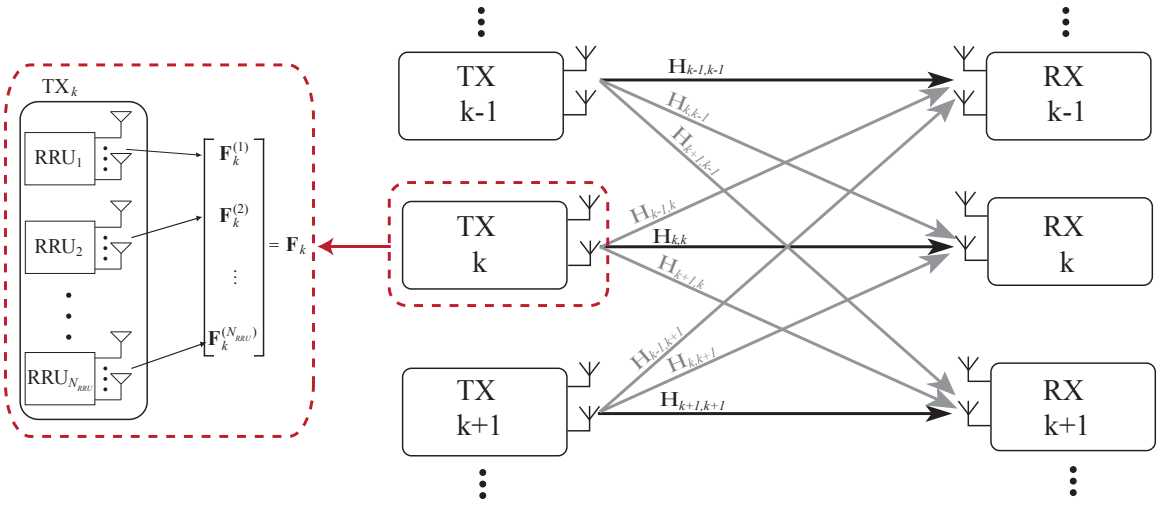


Figure 8: $K$-User MIMO interference channel model with distributed antenna transmitters. Each transmitter consists of $N_{\text{RRU}}$ remote radio units each with $N_{\text{t}}/N_{\text{RRU}}$ antennas.

rithms are an interesting topic for future work, the proposed solution is shown to work well in simulation. Namely, the proposed algorithm avoids the sum-rate loss of power back-off and interestingly achieves the same performance as unconstrained IA.

### 2.3.1 Mathematical Framework and Problem Statement

Consider the $K$-user interference channel shown in Fig. 8 in which transmitter $k$ communicates with its targeted receiver $k$ and interferes with all other receivers $\ell \neq k$. We assume that the system is symmetric, meaning that the number of transmit antennas $N_{\text{t}}$, receive antennas $N_{\text{r}}$, and data streams $N_{\text{s}}$ is the same for all transmitter-receiver pairs. We denote such symmetric systems as $(N_{\text{t}} \times N_{\text{r}},\ N_{\text{s}})^K$. In our DAS setup, we assume that each transmitter's antennas are distributed among $N_{\text{RRU}}$ remote radios, each with $N_{\text{t}}/N_{\text{RRU}}$ antennas as shown in Fig. 8.

Let us define $\mathbf{x}_k$ to be the $N_{\text{s}} \times 1$ symbol vector transmitted by node $k$ with $\mathbb{E}\left[\mathbf{x}_k \mathbf{x}_k^*\right] = \mathbf{I}_{N_{\text{s}}}$, $\mathbf{F}_k$ to be the $N_{\text{t}} \times N_{\text{s}}$ precoding matrix used by transmitter $k$, $\mathbf{H}_{k\ell}$ to be the $N_{\text{r}} \times N_{\text{t}}$ channel from transmitter $\ell$ to receiver $k$, and $\mathbf{z}_k$ to be $N_{\text{r}} \times 1$ vector of i.i.d complex Gaussian noise observed at receiver $k$ with covariance matrix $\sigma^2 \mathbf{I}_{N_{\text{r}}}$. Assuming perfect time and frequency synchronization, user $k$'s received signal, $\mathbf{y}_k$, can be written as

$$\mathbf{y}_k = \mathbf{H}_{kk}\mathbf{F}_k + \sum_{\ell \neq k} \mathbf{H}_{k\ell}\mathbf{F}_\ell + \mathbf{z}_k. \tag{32}$$

To enable the calculation of the IA precoders, however, the channels are assumed to be known perfectly to both transmitters and receivers. In practice, channel knowledge can be obtained by reciprocity or feedback [65, 66].

The precoders $\mathbf{F}_k$ are constrained to satisfy a total power constraint given by $\|\mathbf{F}_k\|_F^2 = P$, where $P$ is the *total transmit power* available at each transmitter. Total available power, however, is not the only constraint on the transmit precoders $\mathbf{F}_k$. Practical power amplifiers and transceiver architectures typically place a limit on the power radiated by *individual*

*antennas* or by *groups of antennas* located at the same RRU. To handle per-RRU power constraints mathematically, we partition the precoders $\mathbf{F}_k$ into $N_{\text{RRU}}$ transmit subfilters $\mathbf{F}_k^{(r)}$ each of size $\frac{N_{\text{t}}}{N_{\text{RRU}}} \times N_{\text{s}}$ such that $\mathbf{F}_k = \left[\mathbf{F}_k^{(1)*}, \mathbf{F}_k^{(2)*}, \ldots, \mathbf{F}_k^{(N_{\text{RRU}})*}\right]^*$ as illustrated in Fig. 8. Constraints are then placed on the Frobenius norm of each subfilter $\mathbf{F}_k^{(r)}$. In cases where *per-antenna* power is restricted, constraints are simply placed on the norm of individual rows $\mathbf{f}_k^{(r)}$ of the precoder $\mathbf{F}_k$ (equivalently RRUs can be thought of as having a single antenna each). With this notation, we define the two power constraints:

1. *Maximum Power Constraints* where the maximum power radiated by an RRU or an antenna is constrained, i.e., $\|\mathbf{F}_k^{(r)}\|_F^2 \leq \frac{P}{N_{\text{RRU}}}$ in the case of per-RRU constraints and $\|\mathbf{f}_k^{(r)}\|_2^2 \leq \frac{P}{N_{\text{t}}}$ in the case of per-antenna constraints.

2. *Strict Power Constraints* where a strict equality constraint is placed on the power radiated by different RRUs or antennas, i.e., $\|\mathbf{F}_k^{(r)}\|_F^2 = \frac{P}{N_{\text{RRU}}}$ in the case of per-RRU constraints or $\|\mathbf{f}_k^{(r)}\|_2^2 = \frac{P}{N_{\text{t}}}$ in the case of per-antenna constraints.

Sections 2.3.2 and 2.3.3 analyze the effects of these more stringent constraints on IA feasibility and performance. When IA's performance is considered, the main metric of interest is the average sum-rate achieved with complex Gaussian signaling and treating interference as noise. Under these assumptions, sum-rate is given by [67]

$$\bar{R}_{\text{sum}} = \mathbb{E}_{\mathcal{H}}\left[\sum_{k=1}^{K} \log_2 \left| \mathbf{I}_{N_{\text{r}}} + \left(\sigma^2 \mathbf{I}_{N_{\text{r}}} + \sum_{\ell \neq k} \mathbf{H}_{k\ell}\mathbf{F}_\ell \mathbf{F}_\ell^* \mathbf{H}_{k\ell}^*\right)^{-1} \mathbf{H}_{kk}\mathbf{F}_k\mathbf{F}_k^*\mathbf{H}_{kk}^* \right|\right], \tag{33}$$

where $\mathbb{E}_{\mathcal{H}}$ denotes expectation over the distributions of the channels $\mathbf{H}_{k\ell}$ $\forall k, \ell$.

While IA can be used with any receiver architecture, alignment can be intuitively understood by examining the operation of a linear interference zero-forcing receiver. Define $\mathbf{W}_k$ to be the $N_{\text{r}} \times N_{\text{s}}$ linear zero-forcing combiner used by receiver $k$. The received signal at the output of $\mathbf{W}_k$ is given by

$$\mathbf{W}_k^*\mathbf{y}_k = \mathbf{W}_k^*\mathbf{H}_{kk}\mathbf{F}_k\mathbf{x}_k + \mathbf{W}_k^* \sum_{\ell \neq k} \mathbf{H}_{k\ell}\mathbf{F}_\ell\mathbf{x}_\ell + \mathbf{W}_k^*\mathbf{z}_k. \tag{34}$$

At the output of $\mathbf{W}_k$, the conditions that ensure perfect alignment can be stated as

$$\mathbf{W}_k^*\mathbf{H}_{k\ell}\mathbf{F}_\ell = \mathbf{0}_{N_{\text{s}}}, \qquad \forall k, \ell \in \mathcal{K},\ k \neq \ell, \tag{35}$$

$$\text{rank}\left(\mathbf{W}_k^*\mathbf{H}_{kk}\mathbf{F}_k\right) = N_s, \qquad \forall k \in \mathcal{K}, \tag{36}$$

where $\mathcal{K}$ is the set of users and $\mathbf{0}_{N_{\text{s}}}$ is the $N_{\text{s}} \times N_{\text{s}}$ all-zeros matrix. Interference alignment and cancellation is guaranteed by (35), and (36) ensures the decodability of user $k$'s desired signal. The IA conditions in (35)-(36) have been used extensively in the literature to derive several IA algorithms [50, 51, 64] and various performance results [60, 62, 65, 66, 68].

The work in [60] leveraged conditions (35) and (36) to characterize the systems in which IA is feasible. The authors of [60] defined the notion of *proper IA systems* in which the

number of free variables in the transmit precoders $\mathbf{F}_k$ always exceeded the number of constraints imposed by condition (35). It was then shown that system properness constitutes a necessary condition for IA feasibility. More recent work has shown that, while properness does not rigorously guarantee IA feasibility, proper systems are most often feasible except in a few corner cases [61, 62]. As a result, the notion of properness can provide a sufficiently accurate predictor of IA feasibility. For the symmetric systems considered in this paper, for example, an IA system is considered proper (and most likely feasible) as long as

$$N_{\mathrm{t}} + N_{\mathrm{r}} \geq (K+1)\, N_{\mathrm{s}}. \tag{37}$$

The conditions in (35)-(36) have similarly been used to derive iterative algorithms in cases where closed form solutions do not exist. In the alternating minimization solution of [51], the total power of *leakage interference*, defined as $\sum_{\ell} \|\mathbf{W}_k \mathbf{H}_{k\ell} \mathbf{F}_{\ell}\|^2$, is iteratively minimized over alternating choices of $\mathbf{F}_{\ell}$ and $\mathbf{W}_k$. Using the derived algorithms, IA was ultimately shown to provide good high-SNR sum-rate in a variety of MIMO interference channels.

Since existing IA algorithms, feasibility results, and performance analysis do not consider per-RRU or per-antenna power constraints, it remains unclear if IA's promise carries over to DAS. To see this, note that algorithms that neglect per-RRU power constraints yield precoders with an unbalanced power profile across different antennas. This power imbalance can be significant in DAS where different antennas experience significantly different pathloss. If maximum power is constrained, transmitters can back-off their *total transmit power* to ensure that no RRU exceeds its power constraint. Power back-off, however, will result in a loss of both effective SNR and IA sum-rate which we characterize analytically in Section 2.3.2. In systems that require all RRUs to transmit at the *same power*, existing IA algorithms cannot be used altogether and power back-off cannot be used to balance RRU transmit power. In fact, Section 2.3.3 shows that placing such strict constraints on per-RRU power significantly affects IA feasibility. For such systems, Section 2.3.3 derives revised properness conditions and provides an iterative algorithm that enables calculating constrained IA precoders.

### 2.3.2 IA Sum Rate loss with Maximum Power Constraints

When a limit is placed on per-RRU transmit power, IA precoders must satisfy the following $N_{\mathrm{RRU}}$ inequality constraints

$$\|\mathbf{F}_k^{(r)}\|_F^2 \leq \frac{P}{N_{\mathrm{RRU}}}, \qquad \forall r \in \mathcal{R},\ \forall k \in \mathcal{K}, \tag{38}$$

where $\mathcal{R}$ is the set of RRUs. Since per-antenna constraints are mathematically equivalent to (38) with $N_{\mathrm{RRU}} = N_{\mathrm{t}}$, we focus on the general case of per-RRU constraints. Examining the IA conditions given by (35) and (36), we note that the constraints in (38) should not affect IA feasibility. Indeed, suppose that there exists a set of precoders $\mathbf{F}_k$ and combiners $\mathbf{W}_k$ that satisfy (35)-(36) with a maximum RRU transmit power of $\beta_k = \max_{r \in \mathcal{R}} \|\mathbf{F}_k^{(r)}\|_F$. In this case, the *scaled* precoders $\frac{\sqrt{P/N_{\mathrm{RRU}}}}{\beta_k}\mathbf{F}_k$ simultaneously ensure that alignment is preserved and transmit power constraints are respected.

While the constraints in (38) do not affect feasibility, satisfying them via power back-off causes a systematic reduction in IA sum-rate since $\frac{\sqrt{P/N_{\mathrm{RRU}}}}{\beta_k} < 1$ with probability one. To

gain a quantitative understanding of the performance degradation induced by power back-off, we examine the mean loss in sum-rate at high SNR which we define in the following proposition.

**Lemma 3** *The mean loss in sum-rate resulting from transmit power back-off at high SNR is given by*

$$\bar{R}_{\text{loss}} = \sum_{k=1}^{K} N_{\text{s}} \mathbb{E}\left[\log_2\left(\frac{P}{N_{\text{RRU}}\beta_k^2}\right)\right]. \tag{39}$$

Given Lemma 3, all that remains to complete the characterization of $\bar{R}_{\text{loss}}$ is to derive the statistics of the random variables $\beta_k^2$. The distribution of $\beta_k^2$, however, is tied to the distribution of the precoders $\mathbf{F}_k$ and is thus dependent (non-trivially) on the statistical model used for the propagation channels $\mathbf{H}_{k\ell}$. This makes deriving the distribution of $\beta_k^2$ for general channel models intractable. Thus, to simplify the rate analysis, we make the following channel assumption.

**Assumption 1** *We assume that all channels $\mathbf{H}_{k\ell}$ are Rayleigh fading, i.e., have i.i.d $\mathcal{CN}(0,1)$ entries.*

Mathematically, Assumption 1 enables us to use the following result from [68].

**Theorem 2** *Assuming Rayleigh-fading channels, the precoders $\mathbf{F}_k \in \mathbb{C}^{N_{\text{t}} \times N_{\text{s}}}$ for $k \in \mathcal{K}$ generated using the IA algorithms in [6, 51, 64] are Haar-distributed, i.e., they are uniformly distributed over the set of orthogonal $N_{\text{s}}$-frames in $\mathbb{C}^{N_{\text{t}}}$.*

Theorem 2 facilitates the derivation of $\beta_k$'s statistics by (i) identifying a single tractable distribution for the precoders $\mathbf{F}_k$, and (ii) consequently indicating that all variables $\beta_k$ are statistically equivalent. As a result, we henceforth drop the subscript $(\cdot)_k$ from $\beta_k$.

For brevity, we give the final results on the distribution of the power back-off factor $\beta$ and refer the reader to [69] for more detailed derivations.

**Proposition 1** *In the case of single stream transmission, i.e., $N_{\text{s}} = 1$, and assuming that $\frac{N_{\text{t}}}{N_{\text{RRU}}}$ is a constant natural number, the CDF of the random variable $\beta^2$ can be approximated as*

$$\mathbb{P}_{\beta^2}\left\{\beta^2 \leq x\right\} \approx \mathcal{Q}\left(N_{\text{t}}x; \frac{N_{\text{t}}}{N_{\text{RRU}}}\right)^{N_{\text{t}}}. \tag{40}$$

*and the approximation can be proven to be exact in the limit of $N_{\text{t}} \to \infty$.*

**Proposition 2** *The distribution of the maximum RRU transmit power $\beta^2$ in the case of $N_{\text{s}} > 1$ can be approximated as*

$$\mathbb{P}_{\beta^2}\left\{\beta^2 \leq x\right\} \approx \mathcal{Q}\left(N_{\text{t}}x; \frac{N_{\text{s}}N_{\text{t}}}{N_{\text{RRU}}}\right)^{N_{\text{t}}}. \tag{41}$$

*and the approximation can again be proven to be exact in the limit of $N_{\text{t}} \to \infty$.*

Having found the distribution of the power back-off factor $\beta^2$ for all $N_{\text{s}} \geq 1$, evaluating the mean loss in sum-rate give in Proposition 3 reduces to a simple one-dimensional integral that can be evaluated numerically. Numerical examples about the loss expected from power back off can be found in [69].

### 2.3.3 IA Feasibility with Strict Power Constraints

To ensure that systems transmit at full power, strict equality constraints can be placed on the IA precoders $\mathbf{F}_k$. Recalling the definition in Section 2.3.1, such constraints can be written as

$$\|\mathbf{F}_k^{(r)}\|_F^2 = \text{trace}\left(\mathbf{F}_k^{(r)}\mathbf{F}_k^{(r)*}\right) = \frac{P}{N_{\text{RRU}}},\ \forall r \in \mathcal{R}, \forall k \in \mathcal{K}. \tag{42}$$

As stated in Section 2.3.2, if per-RRU transmit power is neglected, IA algorithms will generate precoders in which the quantities $\|\mathbf{F}_k^{(r)}\|_F$ are continuous random variables. Thus for existing IA solutions $\|\mathbf{F}_k^{(r)}\|_F^2 \neq \frac{P}{N_{\text{RRU}}}$ with probability one. Unlike maximum power constraints, however, (42) cannot be satisfied via simple transmit power back-off. Further, it is possible that enforcing the strict power constraints in (42) will fundamentally affect the feasibility of IA in DAS and will necessitate the development of improved IA algorithms that explicitly account for per-RRU power.

To explore the reduction in feasibility caused by enforcing strict power constraints, we leverage and extend the notion of properness which was introduced in [60]. Since the MIMO interference channels considered in this paper are symmetric, properness can be determined by examining the number of free variables and unsatisfied equations in the *full set of IA conditions* (35), i.e., there is no need to consider subsets of equations from (35) [60]. Let $N_{\text{v}}$ be the total number of free variables in the IA system, and let $N_{\text{e}}^{(1)}$ and $N_{\text{e}}^{(2)}$ be the number of non-trivially satisfied equations in (35) and (42) respectively.

From [60], the number of free variables $N_{\text{v}}$ and unsatisfied equations $N_{\text{e}}^{(1)}$ in (35) are given by

$$N_{\text{v}} = K(N_{\text{t}} + N_{\text{r}} - 2N_{\text{s}})N_{\text{s}}, \tag{43}$$

$$N_{\text{e}}^{(1)} = K(K-1){N_{\text{s}}}^2. \tag{44}$$

The details of this counting argument are provided in [60]. In short, $N_{\text{v}}$ is determined by counting the free variables in $\mathbf{F}_k\ \forall k \in \mathcal{K}$ and $\mathbf{W}_k\ \forall k \in \mathcal{K}$ after reducing them to their unique basis representations, while $N_{\text{e}}^{(1)}$ is determined by counting the scalar equations in (35). To count the number of non-trivially satisfied equations in (42), we provide the following result.

**Proposition 3** *The number of non-trivially satisfied equations in (42) is given by*

$$N_e^{(2)} = \max\left\{K(N_{\text{RRU}} - N_{\text{s}}), 0\right\}. \tag{45}$$

Combining (43), (44) and (45), the following characterization of system properness for IA with strict per-RRU power constraints can be obtained.

**Theorem 3** *A symmetric IA system with strict per-RRU power constraints is proper, and is thus expected to be feasible, if and only if*

$$(N_{\text{r}} + N_{\text{t}})N_{\text{s}} \geq (K+1){N_{\text{s}}}^2 + \max\left\{(N_{\text{RRU}} - N_{\text{s}}), 0\right\} \tag{46}$$

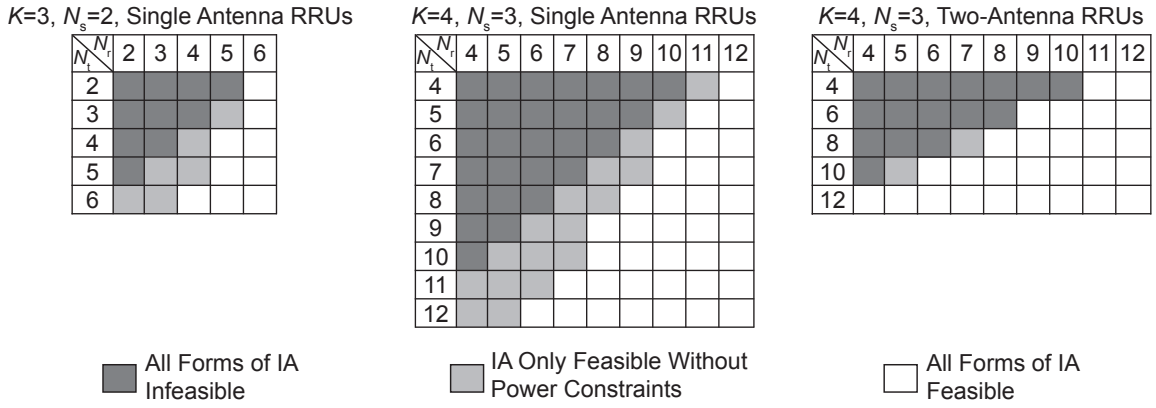


Figure 9: Tables highlighting network configurations in which IA is infeasible, strictly feasible, or feasible only without per-RRU or per-antenna power constraints as predicted by the derived conditions on system properness.

Examining the properness conditions derived in Proposition 3 for IA with strict per-RRU power constraints, we make the following observations:

1. For single antenna RRU's, the properness condition in (46), simplifies to the per-antenna constrained case examined in [59]. Namely, since $N_{\text{RRU}} = N_{\text{t}} \geq N_{\text{s}}$, the condition for properness simplifies to

$$(N_{\text{r}} + N_{\text{t}})N_{\text{s}} \geq (K+1){N_{\text{s}}}^2 + (N_{\text{t}} - N_{\text{s}}). \tag{47}$$

2. Interestingly, per-RRU power constraints only reduce feasibility in cases where $N_{\text{RRU}} > N_{\text{s}}$. In cases where $N_{\text{RRU}} \leq N_{\text{s}}$, the properness condition in (46) reduces to the traditional IA properness condition in (37). As a special case, this regime includes traditional co-located antenna systems ($N_{\text{RRU}} = 1$) with only a total transmit power constraint.

3. Per-RRU power constraints destroy the symmetry of alignment since the properness condition no longer depends on $N_{\text{t}}$ and $N_{\text{r}}$ only through their sum $N_{\text{t}} + N_{\text{r}}$. Therefore, unlike in the traditional IA case explored in [60], if an $(N_{\text{t}} \times N_{\text{r}}, N_{\text{s}})^K$ system is proper and thus likely feasible, the $((N_{\text{t}}+1) \times (N_{\text{r}}-1), N_{\text{s}})^K$ system need not be feasible. The reciprocal $(N_{\text{r}} \times N_{\text{t}}, N_{\text{s}})^K$ system need not be feasible either.

4. Interestingly, in the case of $N_{\text{s}} = 1$ with single antenna RRUs, i.e., $N_{\text{RRU}} = N_{\text{t}}$, transmit antennas are entirely useless for alignment or any transmit-side interference nulling. This can be seen by noting that, in this case, the properness condition simplifies to $(N_{\text{t}} + N_{\text{r}}) \geq (K+1) + (N_{\text{t}} - 1) \implies N_{\text{r}} \geq K$. The condition $N_{\text{r}} \geq K$ implies that the receivers must have enough antennas to single-handedly cancel all unaligned interference and decode their desired signals. Note that in this case, the transmit precoders are simply equal-gain beamforming vectors [54] which we have now shown can never be used for alignment.

**Algorithm 1:** IA with Strict per-RRU Power Constraints

**Input:** $\{\mathbf{H}_{k\ell}\}_{k,\ell=1}^{K}$

**Output:** $\{\mathbf{F}_k\}_{k=1}^{K}$ and $\{\mathbf{W}_k\}_{k=1}^{K}$

Arbitrarily generate initial $\{\mathbf{F}_k\}_{k=1}^{K}$ and $\{\mathbf{W}_k\}_{k=1}^{K}$

**for** a fixed number of iterations **do**

Construct $\{\mathbf{W}_k\}_{k=1}^{K}$ using (49).

Construct $\{\mathbf{F}_k\}_{k=1}^{K}$ using (50).

**for** $\forall k \in \mathcal{K}$ and $r \in \mathcal{R}$ **do**

$\mathbf{F}_k^{(r)} \leftarrow \frac{\sqrt{\frac{P}{N_{\mathrm{RRU}}}}}{\|\mathbf{F}_k^{(r)}\|_F}\mathbf{F}_k^{(r)}$

**end for**

**end for**

**return** $\{\mathbf{F}_k\}_{k=1}^{K}$ and $\{\mathbf{W}_k\}_{k=1}^{K}$

5. The condition in (46) confirms the intuition that having multiple antenna RRUs (such that $N_{\mathrm{RRU}} < N_{\mathrm{t}}$) significantly reduces the effect of per-RRU power constraints and thus improves IA feasibility.

To get a better understanding of the effect of per-RRU power constraints on IA feasibility, Fig. 9 tabulates some example scenarios in which IA is always feasible, feasible *only in the absence of per-RRU power constraints*, or always infeasible,. Comparing the two $K = 4$ cases with single and multi-antenna RRUs, we see that for a fixed number of transmit antennas $N_{\mathrm{t}}$, even as little as two antennas per-RRU can dramatically improve feasibility.

### 2.3.4 Algorithm for IA with Strict Power Constraints

While Proposition 3 gives properness conditions under which IA with strict per-RRU power constraints is expected to be possible, it provides no insight on how to realize such alignment precoders. To better demonstrate the feasibility of IA with per-RRU constraints, we extend the method of alternating minimization used in [51, 64] to provide a simple algorithm which satisfies both the alignment conditions in (35) and the per-RRU constraints in (42).

The alternating minimization strategy used in [51, 64] can be summarized as iteratively minimizing the total power of leakage interference, defined as

$$\mathcal{J}_{\mathrm{IL}}\left(\{\mathbf{F}_k\}_{k\in\mathcal{K}}, \{\mathbf{W}_k\}_{k\in\mathcal{K}}\right) = \sum_{\ell\in\mathcal{K}}\sum_{k\in\mathcal{K}\setminus\ell} \|\mathbf{W}_k^*\mathbf{H}_{k\ell}\mathbf{F}_\ell\|_F^2, \tag{48}$$

over alternating choices of $\mathbf{W}_k$ and $\mathbf{F}_k$. We refer the reader to [51,64] for a detailed derivation of the optimal choice of $\mathbf{W}_k$ and $\mathbf{F}_k$ in each iteration and give the final result here for brevity. At each iteration, the combiners $\mathbf{W}_k$ are chosen as

$$\mathbf{W}_k = \nu_{\min}^{N_{\mathrm{s}}}\left(\sum_{\ell\neq k}\mathbf{H}_{k\ell}\mathbf{F}_\ell\mathbf{F}_\ell^*\mathbf{H}_{k\ell}^*\right), \tag{49}$$

followed by an update to the choice of precoders given by

$$\mathbf{F}_k = \nu_{\min}^{N_s}\left(\sum_{\ell \neq k} \mathbf{H}_{\ell k}^* \mathbf{W}_\ell \mathbf{W}_\ell^* \mathbf{H}_{\ell k}\right), \tag{50}$$

where $\nu_{\min}^{N_s}(\cdot)$ denotes the $N_s$ least dominant eigenvectors of a symmetric matrix. To satisfy the per-RRU power constraints, we add a projection step onto the set of precoders with a fixed RRU transmit power of $\frac{P}{N_{\text{RRU}}}$. The projection on that set amounts to scaling and updating the blocks of $\mathbf{F}_k$ as

$$\mathbf{F}_k^{(r)} \leftarrow \frac{\sqrt{\frac{P}{N_{\text{RRU}}}}}{\|\mathbf{F}_k^{(r)}\|_F}\mathbf{F}_k^{(r)}. \tag{51}$$

The steps of the algorithm are listed more formally in Algorithm 1.

### 2.3.5 Intuition Obtained from the Results

Our results indicate that distributed antennas are an attractive system-level solution to increase the utility of IA in practical wireless systems. While maximum power constraints may reduce sum-rate relative to unconstrained IA, and strict power constraints may reduce feasibility, the system configurations we considered showed promising sum-rate performance for most users in a wireless network. As a result, the SNR boost provided by DAS is sufficient to justify the "reduced" sum-rate and feasibility. Further, we showed that existing IA algorithms can be extended to systems with per-radio power constraints, thus the performance demonstrated in theory can be achieved by practical iterative algorithms. In conclusion, our work proves that the combination of IA and DAS can improve data rates for the majority of mobile users when compared to (i) IA in systems with co-located antennas, and (ii) distributed antennas with existing interference management solutions.

## 2.4 Prototyping MIMO Interference Alignment

Most prior work on IA makes assumptions about perfect synchronization and CSI at the transmitter (CSIT), which is not realistic. To overcome these issues, we developed a prototype of interference alignment that operates in a completely distributed fashion, with each node performing estimation and synchronization.

CSI feedback quality was studied with limited feedback [66] and analog feedback [37]. The impact of feedback combined with imperfect channel estimation was established in [70]. In [70], it is assumed that the CSI feedback is given with analog feedback, and IA's performance with imperfect feedback is analyzed with the CSI errors caused by the channel estimation error in feedforward channel, the channel estimation error in feedback channel, and the decoding error of CSI data in feedback channel. A main conclusion is that analog feedback is a good option for implementing interference alignment. Consequently we incorporate analog interference alignment into our prototype.

There has been limited work on IA from an experimental perspective, essentially reported in [71–73] and [11], IA prototypes are built and the performance of IA is measured and studied from them. In [71], the feasible setups for IA for wireless LAN system and the imperfect

practical issues such as synchronization errors are studied. In [72], the wireless channel is measured from the authors' prototype, and the sum rate is calculated from it mainly showing that the gain in sum rate achieves under the measured channel. In [73], including our initial results reported in [11], the CSI is measured at the receivers, precoding vectors are obtained with the CSI, and the sum rate is calculated from over-the-air precoded transmission.

The main contribution of our work is the first implementation and measurement of real-time distributed IA system. Though there has been prior experimental work, none has considered the practical issues when the nodes of IA are physically distributed, and consequently the system experiences overhead and loss of accuracy when sharing CSI. In our prototype, we implemented over-the-air time and frequency synchronization and feedback mechanisms to achieve this goal. From the prototype, the sum rate was measured showing that IA has a significant gain over the issues. Other measurements were performed considering the accuracy of IA solution, synchronization and CSI feedback mainly showing the relationship between overhead and performance.

### 2.4.1 Mathematical Framework and Problem Statement

Our system models the K-user interference channel. For the interference channel, there is one by one mapping of a transmitter and a receiver. Only the data streams from $i$-th transmitter is the desired streams to $i$-th receiver, and the streams from the other transmitters are the interfering streams. Each of the transmitters and the receivers has $N_t$ and $N_r$ antennas respectively, and all nodes are separated. Our hardware uses $N_t = N_r = 2$.

IA basically assumes perfect synchronization and perfect CSI measurement and feedback, which are not feasible in real world. The requirement for time and frequency synchronization for IA is studied in [71]. It is known from [71] that the phase offsets caused by time and frequency synchronization errors are not a problem for IA. The reason is that the phase error in synchronization does not affect the antenna subspaces where IA works. Besides this requirement in synchronization, a protocol for over-the-air nodes' synchronization is required for the distributed system.

There are two types of synchronization for the distributed IA system: synchronization among transmitters and synchronization between the transmitter side and the receiver side. Once the former is achieved, then the latter becomes a point to point synchronization that is well studied in literature. Thus, most of the effort in our prototype was spent on synchronization among the transmitters.

For our interference channel model, all the transmitters use the same time and frequency resources to send their own streams, so the multiple streams are overlapped at the receivers. If the transmitters are asynchronous, then the receivers have to estimate and compensate for different time and frequency offsets for each of the transmitted streams, and it is an expensive task for the receivers as an example of asynchronous multiuser MIMO system in [74]. Otherwise, if the transmitters are globally synchronized, the receivers need to estimate and compensate only the global time and frequency offsets for all the overlapped streams, and it has lower synchronization overhead than the case of the asynchronous transmitters.

For the transmitter synchronization, master-slave synchronization protocols have been proposed in [75, 76] and [77]. In [75], a precise symbol-level time synchronization protocol is introduced for wireless LAN systems, and in [76] a frequency synchronization method based

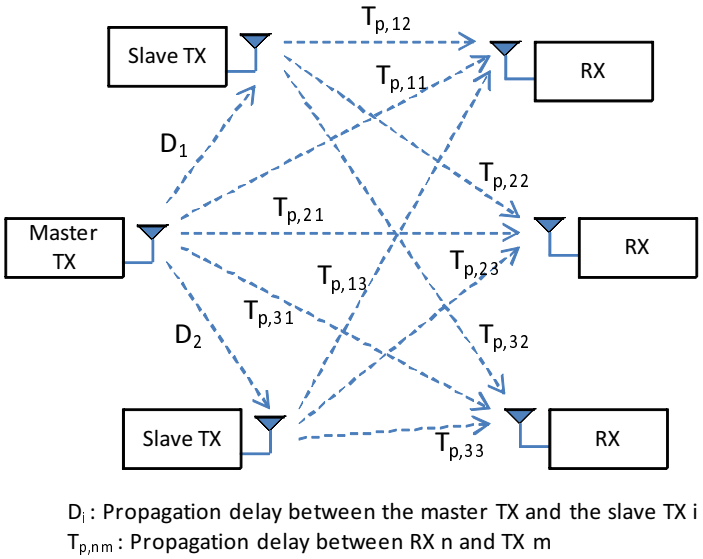


(a) System with different propagatin delays.

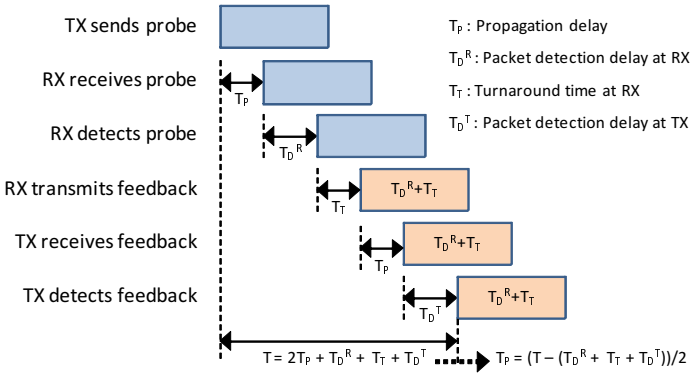


(b) Acquisition of one propagation delay.

Figure 10: Over-the-air master-slave synchronization protocol.

on the time synchronization protocol in [75] is also presented. Fig. 10(a) shows an example of the system that has different propagation delays between any two nodes. The protocol in [75] assumes different propagation delays. One of the transmitters works as the master transmitter while others become the slave transmitters. The goal is to align the transmitters in time and frequency so that the signals from all the transmitters arrive as close as possible in time and frequency at the receivers.

To acquire the propagation delays and the other internal delays, each of the transmitters periodically sends a probe to the others. Fig. 10(b) shows the possible delay elements and the method how to obtain them. Once transmitter sends the probe (this transmitter is denoted as 'TX' in Fig. 10(b)), and then each of the other transmitters and the receivers (denoted as 'RX' in Fig. 10(b)) senses the probe, measures the internal processing delay to detect the probe ($T_D^R$) and the turnaround delay from receiving mode to transmitting mode ($T_T$), informs the sum of those delays back to the transmitter that sends the probe. Then, the transmitter receives this feedback from each of the nodes, and measures the air propagation

delays ($T_P$) with its internal detection time ($T_D^T$) and the delay information ($T_D^R + T_T$) given by the feedback node. The other transmitters perform the same task in turn.

When all the required delay information is obtained, the system is ready to work in synchronous manner. The master transmitter sends its training to the other transmitters, and each of the other transmitters adjusts the time with the previously measured delay information to send its own packet. After some time margin to this adjustment, all transmitters send their synchronized packets to the receivers. If multiple receivers exist in the system, however, it is impossible to make all receivers receive the transmitters' signals at the exactly same time. Instead, the transmitters adjust their packet transmission time so that the sum timing error at all the receivers is minimized, e.g. all the signals are to be received within the cyclic prefix of orthogonal frequency division multiplexing (OFDM) system.

For frequency synchronization, the slave transmitters measure the frequency offset with the master's training, recover the offset before they send their data packet [76]. Along with the frequency offset, the phase offset between the master and the slaves are also considered in [76]. The phase offset caused by oscillator offset is inevitable, and it may affect the performance of wireless systems. To enable the slaves to measure the phase difference from the master, two identical trainings are sent from the master : one at the first transmission of the synchronization training and the other at actual data transmission. The slaves detect these two trainings and compare them to estimate phase offset between two. If the residual frequency offset is small, it can be assumed that there is only the constant phase offset between the master and a slave. The slaves also compensate the phase offset before their data transmission.

In [75, 76], TDD is assumed, but there is also a scheme that assumes frequency division multiplexing (FDD) and continuous transmission [77]. In [77], the master continuously sends its OFDM-based training to the slaves via a dedicated synchronization channel, and the phase rotation of OFDM subcarriers caused by time and frequency offset from the master is measured and compensated by the slaves before they send their own data stream.

For CSI feedback, there are three major error types: the error caused by AWGN, the limited feedback error, and the delayed feedback error. The limited feedback error occurs because of the quantization of the estimated CSI, while the delayed feedback error is by channel's time-varying property. IA with limited feedback is first analyzed in [66]. In [66], the CSI quantization error with Grassmannian codebook [78] is analyzed assuming perfect CSI measurement and feedback. According to its result, the DOF of $K/2$ for single input and single output IA system is achievable if the number of total feedback bits is larger than $K(L-1)logP_f$, where $L$ is the number of multipaths in feedforward channel and $P_f$ is the trasnmit power of CSI feedback.

Our prior work on analog feedback with IA is presented in [37] as a way to flexibly implement feedback in a way that avoids quantization error. In [37], the feedback channel's estimation error by AWGN at feedback training and the feedback data error caused by AWGN at data symbols are considered. It is shown that the multiplexing gain of IA is preserved only with a constant sum rate loss when the transmitting power of feedback linearly relates to the transmitting power of feedforward. The upper bound of the constant sum rate loss $\Delta R_{sum}$ is given as the function of the length of the training for feedback channel estimation ($\tau_p$), the length of the CSI feedback ($\tau_c$), and the ratio of $P_f$ and the transmit

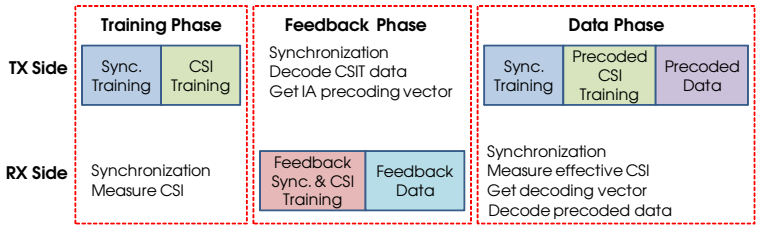


Figure 11: Operation scenario for the prototype.

power $P$ of feedfoward channel:

$$\Delta R_{sum}(\tau_p, \tau_c) \leq \sum_i d_i log_2(1 + \frac{P}{P_f} c(\tau_p, \tau_c)(K - \frac{1}{d_i})). \tag{52}$$

where $c(\tau_p, \tau_c)$ is a value that depends on $\tau_p$ and $\tau_c$, and if either $\tau_p$ or $\tau_c$ gets larger, $c(\tau_p, \tau_c)$ gets smaller showing that with more overhead in the feedback channel estimation training and feedback data, the sum rate loss $\Delta R_{sum}$ gets smaller. To maintain the multiplexing gain, $P_f$ needs to linearly scale with $P$, i.e. $P_f = \alpha P$. Otherwise, if $P_f$ is not linear with $P$ as $P_f = \alpha P^\beta$, there exists a loss in multiplexing gain according to $\beta$. A similar extended study also considering the feedforward channel estimation error is presented in [70].

### 2.4.2 System Realization

We are targeting $2 \times 2$ MIMO three user IA system. $N_t = N_r = 2$ for all user pairs, $N_s = 1$, and $K = 3$. OFDM is used for both feedforward and feedback channels. With this setup, two antenna subspaces are available for a user pair, and two interfering streams are aligned in one subspace at each receiver while the desired stream is received in the other subspace. Both the closed form solution and the iterative method in [79] are implemented in our prototype.

There are three main phases in IA operation scenario: training, feedback and data phases. Fig. 11 summarizes the signals that are needed to be transmitted at each of the phases, and also shows the tasks that should be done during each of the phases at the transmitters and the receivers.

- **Training Phase**: This is mainly for CSI measurement at the receivers. The synchronization training is sent from the transmitters followed by the CSI training. The receivers first synchronize to the transmitters in time and frequency with the received synchronization training, and then measure CSI which should be given back to the transmitters at the feedback phase. Furthermore, the synchronization among the transmitters should be done at this phase. The details about the training structure and the transmitter synchronization is given in the following section.

- **Feedback Phase**: This phase is for CSI feedback. Each of the receivers makes a packet which is consisted of the synchronization training, the CSI training, and the CSI feedback data, and the packet is sent to the transmitters via over-the-air transmission. The packets are sent in time orthogonal manner. After receiving and decoding these packets, the transmitters calculate IA precoding vectors.

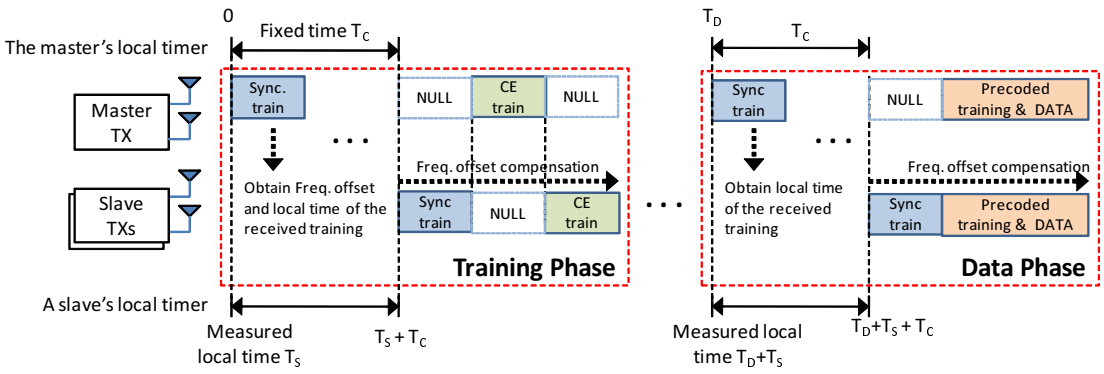


Figure 12: Transmitter synchronization in our prototype.

- **Data Phase**: This phase is for the precoded training and data transmission. The synchronization training, the precoded CSI training, and the precoded data are sent to the receivers in order. The receivers first synchronize to the transmitters, calculate the decoding vectors with the precoded CSI training, and decode the precoded data with them. Finally, the sum rate is calculated and the operation ends.

The master-slave protocol is used for over-the-air transmitter synchronization in our prototype, but there are two differences from the algorithms in [75] and [76]. First of all, the phase synchronization in [76] is not required in our prototype since it does not affect IA performance. Also, time synchronization is simplified from [75]. The over-the-air propagation delays between nodes are assumed to be the same. With this assumption, there is no need to measure the air propagation delays. Then, the processing delay and the turn-around delay at both the transmitters and the receivers do not matter only if the following two requirements are guaranteed : 1) a symbol should be sent from transmitting antennas exactly at desired time at the transmitters, and 2) the exact time when a symbol arrives to receiving antennas is known at the receivers. These requirements are supported by our implementation hardware and software.

Fig. 12 illustrates our protocol. For our distributed system, it is assumed that each of the nodes are physically separated, and this means that every node works with its own time and frequency references not knowing the others' references. At the training phase which is the starting point of one turn of IA procedure, the synchronization is done in the following three steps:

- Step 1. The master transmitter first sends its training to the slave transmitters at time zero with its local timer. When each of the slaves receives and detects the training, it knows its local time $T_S^{[n]}$ when the first sample of the training is arrived at its antennas. Here, $n$ is the slave index. The slaves also measure the frequency offset from the master's frequency with this training.

- Step 2. $T_C$ is the waiting time for synchronized transmission, and it is known to all transmitters. The master and the slaves wait until their local time reaches $T_C$ for the master, and $T_S^{[n]} + T_C$ for the slaves.

- Step 3. All the transmitters send their own training to the receivers immediately when their waiting time ends. Each of the slaves recovers the measured frequency offset from its own training before it is sent. The training and data are now synchronized in time and frequency.

The same operation is performed at the data phase since the time between the training phase and the data phase may not short enough for the slaves to maintain their previous synchronization. At the data phase, the starting time of the data phase, $T_D$, is only known to the master and it sends its training again to the slaves at that time. The slaves now detect it at time $T_S^{[n]} + T_D^{[n]}$, and all transmitters send the synchronization training and data after $T_C$ time. Besides the transmitter synchronization, the receivers also need to synchronize to the transmitters. Each receiver synchronizes independently to the transmitters, and there is no cooperative synchronization among the receivers. The auto-correlation method in [80] is used for synchronization at all nodes.

The main feedback scheme in this paper is analog feedback. Under the assumption of flat fading channel, receiver $i$ measures

$$\mathbf{H}_{ij}, \quad j = 1, 2, 3. \tag{53}$$

Since each $\mathbf{H}_{ij}$ is $2 \times 2$ matrix, there are $K \times N_t \times N_r$ complex values for the measured CSI at each receiver. These values are mapped to $N_{sc}$ subcarriers by $N_{sc} \times (K \times N_t \times N_r)$ mapping matrix, and the $N_{sc}$ subcarriers form an OFDM symbol. As a result, each receiver has an OFDM symbol for analog feedback. The transmitters that receive the OFDM symbols apply the pseudo inverse of the mapping matrix to the received OFDM symbols, and find the CSI values. The transmit power which decides the difference in SNR between feedforward and feedback channel as in (52) is a design parameter.

For limited feedback as a competitor, the explicit feedback beamforming method from the beamforming specification of 802.11n wireless LAN is used [81]. With the quantization method, $N_{gain}$ bits are used for the amplitude of CSI, and $N_q$ bits are used to quantize each of real and imaginary values of the measured CSI. $N_{gain} = 3$ and $N_q = 4, 5, 6$ and 8 for our implementation. $G_{ref}$ is chosen to minimize the mean squared error (MSE) by quantization. Note that this is really a brute force quantization technique and is not "limited" in any sense.

### 2.4.3 Experiments and Results

Table 1: OFDM parameters for the prototype.

| | |
|---|---|
| FFT length | 128 |
| Cyclic Prefix Length | 32 |
| Number of null subcarriers | 23 |
| Number of data subcarriers | 105 |

The system is designed to operate at 2.4 GHz, the bandwidth would ideally be large as 20 MHz, but it is lower as 1 MHz in our prototype because of hardware constraints. Both feedforward and feedback channel use the same frequency, and the system is a TDD system.

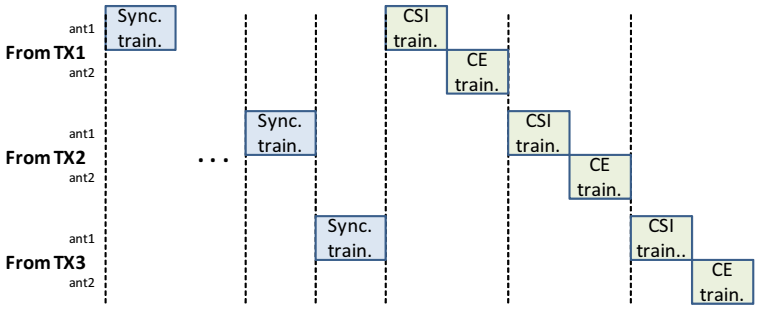


(a) Feedforward packet structure for training phase.

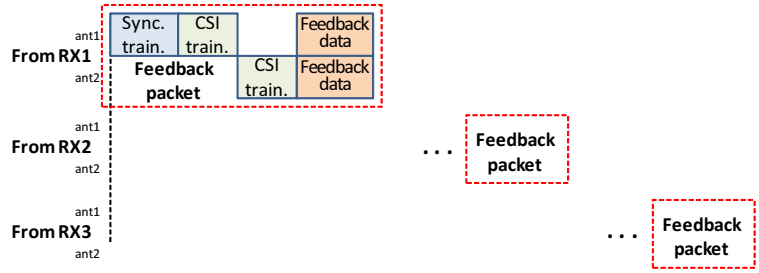


(b) Feedback packet structure.

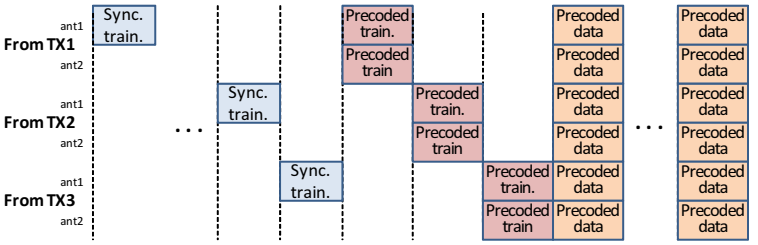


(c) Feedforward packet structure for data phase.

Figure 13: Packet structures.

OFDM is used for the training and data, and only the synchronization training is generated at time domain. The OFDM parameters are summarized in Table 1.

As described in the previous sections, our system works in three phases : the training, the feedback and the data phases. For each of the phases, the packet structure is shown in Fig. 13. In Fig. 13, the packet structures for the training phase (Fig. 13(a)), the feedback phase (Fig. 13(b)), and the data phase (Fig. 13(c)) are given. There are three types of trainings in our system:

- **Synchronization training**: The synchronization training is for the nodes' synchronization. It has two parts : short training for coarse time synchronization and long training for fine time and frequency synchronization. A length 17 Zadoff-Chu sequence is repeated five times as the short training, and a length 29 Zaduff-Chu sequence is repeated three times as the long training. The training has repeated patterns in time domain, and the synchronization is done by the auto-correlation method in [80].

- **CSI training**: The CSI training is for CSI measurement to be sent back to the transmitters for IA precoding vector calculation. One CSI training is an OFDM symbol,

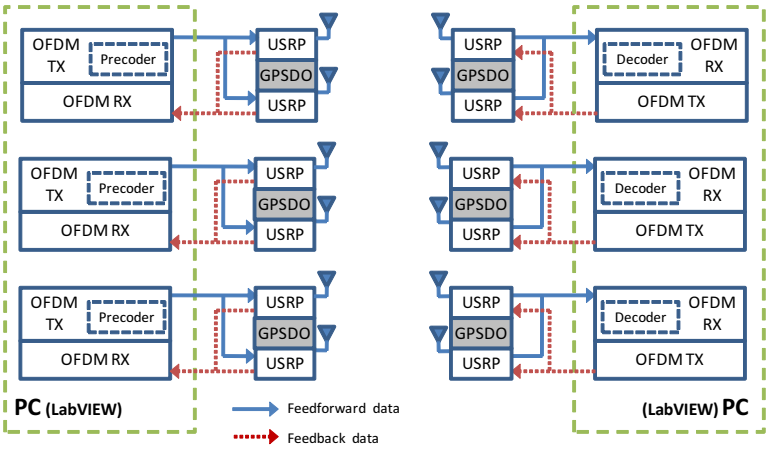


Figure 14: Software and hardware configuration of the prototype.

and it is sent from each of the transmitting antennas in time orthogonal manner as in Fig. 13(a). As such, six OFDM symbols are transmitted for our three user $2 \times 2$ MIMO system. The training does not experience precoding nor decoding. Thus, the receivers can find the pure condition of current wireless channel. With this training, each receiver measures $2 \times 6$ CSI matrix.

- **Precoded training**: The precoded training is sent at the data phase. It experiences IA precoding at the transmitters, where each user in our three user system has one data stream that is mapped to two antennas via the precoding vector. It is used for the decoding vector calculation. Also, since this training is precoded in the same way with the precoded data, it is used to equalize the data symbols. The training is also an OFDM symbol, and it is sent from two transmitting antennas of a transmitter at a time. Each transmitters sends it in time orthogonal manner as in Fig. 13(c).

Fig. 14 shows the hardware and software configuration of our prototype. The system uses two computers that are equipped with dual-core Intel Xeon 2.67 GHz processors and 12GB of memory. One computer is used to control the transmitters, and the other is for the receivers. National Instruments (NI) USRP-2921 [82] is used for analog to digital convertor (ADC) / digital to analog convertor (DAC) and radio frequency (RF) front-end. One USRP works as one antenna, so two USRPs are used for a node, and accordingly one computer controls six USRPs. A USRP can switch between transmitting mode and receiving mode, e.g. the USRPs for the transmitters work in transmitting mode for the training and data phases, but in receiving mode for the feedback phase. The computer and the USRPs are connected via TCP/IP connections. National Instruments (NI) LabVIEW which is a model-based digital signal processing implementation software [83] is used for our software defined radio (SDR) implementation. The control of USRPs is also done by LabVIEW's USRP driver. Though only one computer is used for all the transmitters, and similarly only one computer is used for all the receivers, the signal processing for each node is completely separated from each other not to violate the interference channel model, i.e. there are three parallel independent processing chains in LabVIEW on a computer.

Since our system is distributed system, each node should work with its own oscillator.

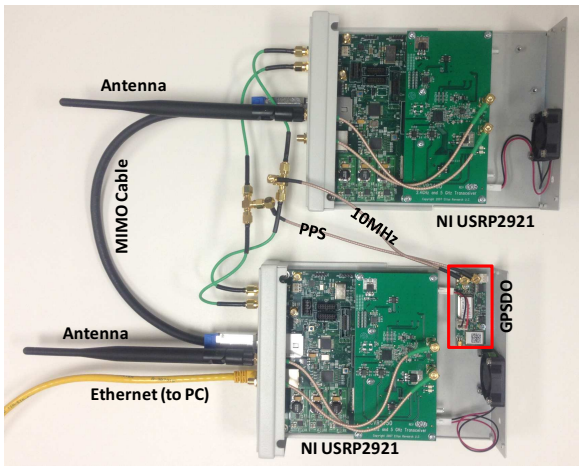


Figure 15: Hardware configuration of one node.

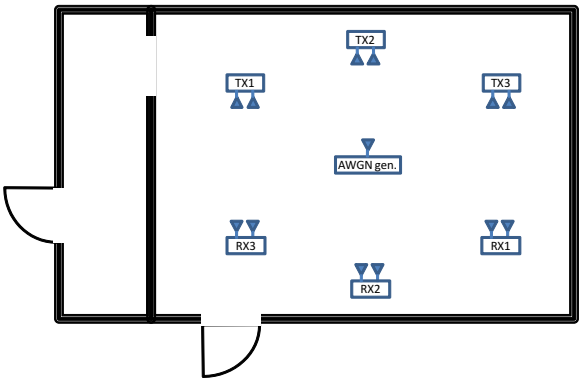


Figure 16: Test environment of distributed nodes.

The GPS disciplined oscillator (GPSDO) module that can be attached to USRP is used as the oscillator for a node [84]. The GPSDO is originally for the global synchronization to the GPS signal which is only available at outdoors. There is, however, no assumption of outdoor operation for IA system in general, so the GPSDOs are not used to synchronize to the global GPS signal. Instead, a GPSDO is used to provide time and frequency references only to a single node in our prototype. Though the GPSDOs are used, our distributed synchronization algorithm is designed assuming that each of the GPSDOs generates the independent time reference (pulse per second (PPS)) and frequency reference (10MHz) without being synchronized to the GPS signal since our prototype is tested in indoor environment where the global GPS signal is unavailable. The PPS and 10MHz are the required time and frequency references for the USRPs respectively. Six GPSDOs are used because there are six nodes in the system, and the time and frequency reference signals from a GPSDO are only shared between two USRPs which form a node's two antennas. Fig. 15 shows the hardware configuration of a node in the prototype. The MIMO cable between the USRPs in Fig. 15 is only used for the ethernet connection of two USRPs to a computer.

Fig. 16 shows the schematic of distributed test environment. Both the transmitters and the receivers are physically separated to verify our system. To make the SNRs of the air

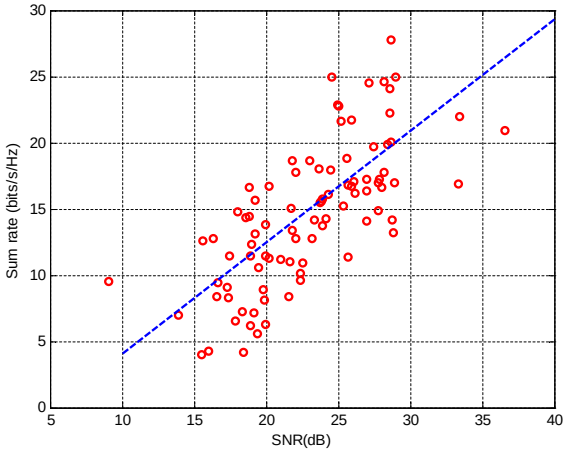


(a) Measured sum rate of distributed IA with analog feedback.

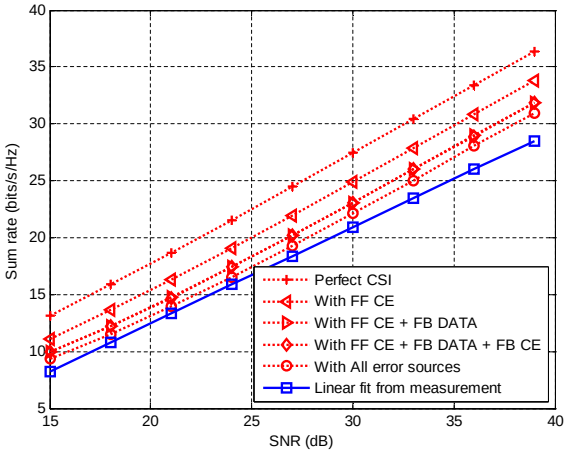


(b) Comparison of measured sum rate to simulated sum rate.

Figure 17: IA performance with analog feedback

links be similar as possible, the distances between any transmitter and any receiver are made to be the same as possible. Also, the AWGN generator which is used to scale the overall SNR of the system is located at the center of the nodes.

In this paper, the sum rate of distributed IA with analog feedback is first presented. Then, more detailed measurements on the relationship between the accuracy of IA solution, residual frequency offset, and CSI feedback are also given. For all the results in this paper, the distributed nodes' synchronization protocol is applied.

The sum rate of our system is given in Fig. 17. Each dot in the first subfigure is the measured instantaneous sum rate within SNR range from 15dB to 35dB and the solid line shows their linear fitting, and the second subfigure shows the comparison of the linear fitting to the simulation results. The simulation is performed under different setups : 1) perfect CSI estimation (CE) and feedback, 2) only with feedforward CE error, 3) with feedforward

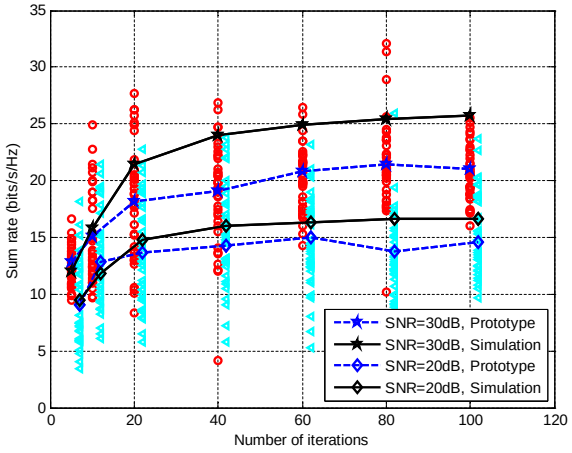


Figure 18: Sum rate with iterative IA method.

CE and feedback data errors, 4) with the errors in 3) and feedback CE error, and 5) with all the error sources : feedforward CE error, feedback data error, and feedback CE error, and feedforward precoded CE error. It is observed from Fig. 17 that the multiplexing gain is maintained by analog feedback only with a constant sum rate degradation if the feedback transmit power is linear to the feedforward transmit power for CSI measurement as analyzed in [37]. This result is possible since the SNRs for feedforward channel and feedback channel are the same in our experiments.

To study the performance with imperfect IA solution, Fig. 18 shows the sum rate versus the number of iterations for the iterative IA method. The iterative method from [79] is used, and the number of iterations is an important design parameter for the method. The mean sum rate at SNR = 30dB and SNR = 20dB are measured and compared to those from the simulation with the perfect CSI feedback. Though the sum rate from the prototype is smaller than that from the simulation because it is limited by CSI estimation and feedback, the number of iterations to achieve the sum rate is not reduced. This shows that the leakage from the imperfect IA solution is independent to the other error sources regardless of SNR of the system.

Fig. 19 shows the IA performance with synchronization error. The time synchronization error of IA with OFDM does not affect the IA performance only if the timing synchronization is done only within cyclic prefix, and this requirement is not new to IA. Frequency synchronization, however, can not be perfect in the real systems, and there always remains the residual frequency offset after synchronization. It causes inter channel interference (ICI) which can not be recovered by IA, so it is added as an extra error source to the system. Furthermore, the ICI by the residual frequency offset affects all the CSI measurement and feedback steps which are listed in Fig. 17. In Fig. 19, the sum rate is plotted with different % frequency offsets with respect to the subcarrier spacing. The same frequency offset is added to the air links between the master transmitter and the slave transmitters, and to the connection between the transmitters and the receivers. The SNR is 30dB.

The analog feedback is also compared to limited feedback. For limited feedback, the uncompressed explicit scalar quantization in 802.11n specification [81] is used as described

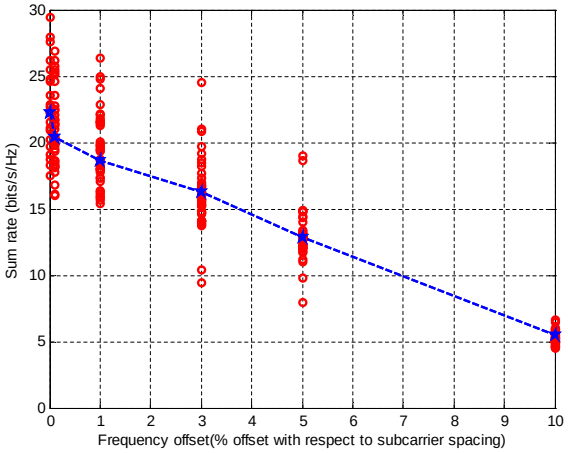


Figure 19: IA performance with the residual frequency synchronization error

in the previous section. $N_q = 4, 5, 6$ and 8 are applied for the evaluation. It is observed from Fig. 20(a) that the slope of sum rate increases as more bits are allocated, i.e. as feedback overhead is increased, which means more bits are needed as feedback as SNR gets high to get the multiplexing gain of IA. Fig. 20(b) shows the sum rate against MSE of limited feedback. The fitting line is the linear connection of the means of the sum rates with different $N_q$. The results in Fig. 20 gives us some interesting observations. First of all, the multiplexing gain of quantization-based feedback increases with increasing number of $N_q$, which corresponds to the previous analysis in [66]. Furthermore, compared to the quantization-based feedback, analog feedback has higher sum rate performance at high SNR region than the quantization-based feedback. This is because the MSE of analog feedback is reduced with increasing feedback SNR, but the MSE of quantization-based feedback is fixed regardless of SNR if it is assumed that there is no bit error for quantization-based feedback.

### 2.4.4 Intuition Obtained from the Results

We implemented a prototype of a three user IA system with $2 \times 2$ antenna configuration for each user. The prototype is fully distributed and uses wireless both for direct communication and feedback. With the prototype, the performance of IA with the practical issues was studied, with an emphasis on the feedback quality. The nodes were assumed to be physically separated and to work independently without cooperation following the basic assumption of interference channel. The distributed operations were achieved by developing over-the-air time and frequency synchronization protocol and feedback methods. Our results show that it is possible to implement IA in a distributed fashion. Further, they show the efficacy of analog feedback in a real-world setting. This means it is a viable approach for achieving good performance as an alternative to quantization based approaches. Finally, we confirmed that there is a lot of overhead associated with the protocol used for distributed synchronization. More work is needed in the future to design a MAC protocol that allows fast setup of distributed IA clusters.

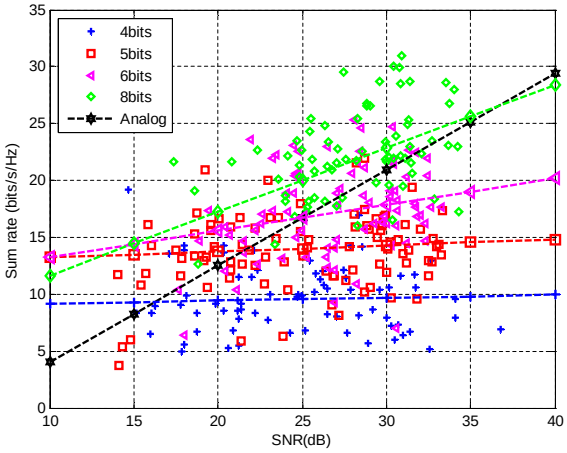


(a) Measured sum rate with limited feedback and analog feedback

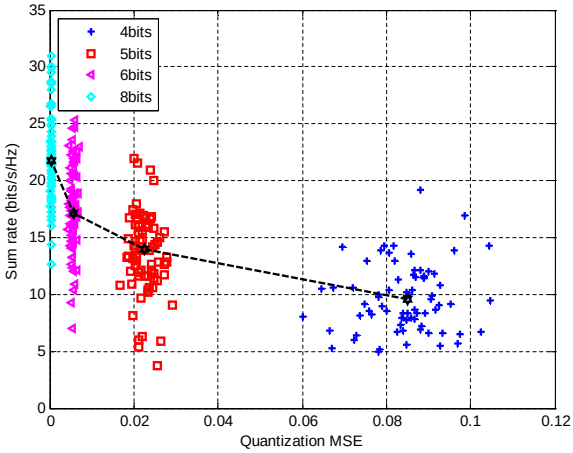


(b) Sum rate vs. MSE of limited feedback.

Figure 20: IA performance with limited feedback

# References

[1] C. E. Shannon, "Two-way communication channels," in *Proc. 4th Berkeley Symposium on Mathematical Statistics and Probability*, vol. 1, Berkeley, CA, July 1961, pp. 351–384.

[2] H. Sato, "The capacity of the Gaussian interference channel under strong interference," *IEEE Transactions on Information Theory*, vol. 27, no. 6, pp. 786–788, Nov. 1981.

[3] A. Carleial, "A case where interference does not reduce capacity," *IEEE Transactions on Information Theory*, vol. 21, no. 5, pp. 569–570, Sept. 1975.

[4] T. Han and K. Kobayashi, "A new achievable rate region for the interference channel," *IEEE Transactions on Information Theory*, vol. 27, no. 1, pp. 49–60, Jan. 1981.

[5] H. F. Chong, M. Motani, H. K. Garg, and H. E. Gamal, "On the Han-Kobayashi region for the interference channel," *IEEE Transactions on Information Theory*, vol. 54, no. 7, pp. 3188–3194, July 2008.

[6] V. R. Cadambe and S. A. Jafar, "Interference alignment and degrees of freedom of the $K$-user interference channel," *IEEE Transactions on Information Theory*, vol. 54, no. 8, pp. 3425–3441, Aug. 2008.

[7] M. A. Maddah-Ali, A. S. Motahari, and A. K. Khandani, "Communication over MIMO $X$ channels: interference alignment, decomposition, and performance analysis," *IEEE Transactions on Information Theory*, vol. 54, no. 8, pp. 3457–3470, Aug. 2008.

[8] R. H. Etkin, D. N. C. Tse, and H. Wang, "Gaussian interference channel capacity to within one bit," *IEEE Transactions on Information Theory*, vol. 54, no. 12, pp. 5534–5562, Dec. 2008.

[9] B. Nosrat-Makouei, J. Andrews, and R. Heath, "User arrival in mimo interference alignment networks," *IEEE Transactions on Wireless Communications*, vol. 11, no. 2, pp. 842–851, 2012.

[10] J. Starr, O. El Ayach, and R. w. Heath Jr., "Interference alignment in distributed antenna systems," Submitted to the IEEE Transactions on Signal Processing.

[11] J. Massey, J. Starr, S. Lee, D. Lee, A. Gerstlauer, and R. Heath, "Implementation of a real-time wireless interference alignment network," in *Signals, Systems and Computers (ASILOMAR), 2012 Conference Record of the Forty Sixth Asilomar Conference on*, 2012, pp. 104–108.

[12] K. Gomadam, V. R. Cadambe, and S. A. Jafar, "Approaching the capacity of wireless networks through distributed interference alignment," in *Proc. IEEE Global Telecommunications Conference*, New Orleans, LA, Nov. 2008, pp. 1–6.

[13] D. S. Papailiopoulos and A. G. Dimakis, "Interference alignment as a rank constrained rank minimization," in *Proc. IEEE Global Telecommunications Conference*, Miami, FL, Dec. 2010, pp. 1–6.

[14] R. T. Krishnamachari and M. K. Varanasi, "Interference alignment under limited feedback for MIMO interference channels," in *Proc. IEEE International Symposium on Information Theory*, Austin, TX, June 2010, pp. 619–623.

[15] O. Ayach and R. Heath, "Interference alignment with analog csi feedback," in *MILITARY COMMUNICATIONS CONFERENCE, 2010 - MILCOM 2010*, 2010-nov.3 2010, pp. 1644 –1648.

[16] A. Ghosh, J. Zhang, J. G. Andrews, and R. Muhamed, *Fundamentals of LTE*. Prentice Hall, 2010.

[17] S. W. Peters and R. W. Heath, Jr., "Orthogonalization to reduce overhead in MIMO interference channels," in *Proc. International Zurich Seminar on Communications*, Zurich, Switzerland, Mar. 2010, pp. 126–129.

[18] C. M. Yetis, T. Gou, S. A. Jafar, and A. H. Kayran, "On feasibility of interference alignment in MIMO interference networks," *IEEE Transactions on Signal Processing*, vol. 58, no. 9, pp. 4771 –4782, Sept. 2010.

[19] D. J. Love, R. W. Heath, Jr., W. Santipach, and M. L. Honig, "What is the value of limited feedback for MIMO channels?" *IEEE Communications Magazine*, vol. 42, no. 10, pp. 54–59, Oct. 2004.

[20] B. Nosrat-Makouei, J. G. Andrews, and R. W. Heath, Jr., "User arrival in MIMO interference alignment networks," *IEEE Transactions on Wireless Communications*, vol. 11, no. 2, pp. 842–851, Feb. 2012.

[21] E. Matskani, N. Sidiropoulos, Z. quan Luo, and L. Tassiulas, "Convex approximation techniques for joint multiuser downlink beamforming and admission control," *IEEE Transactions on Wireless Communications*, vol. 7, no. 7, pp. 2682–2693, July 2008.

[22] P. H. Schönemann, "A generalized solution of the orthogonal Procrustes problem," *Psychometrika*, vol. 31, no. 1, pp. 1–10, 1966.

[23] E. J. Candes and T. Tao, "Decoding by linear programming," *IEEE Transactions on Information Theory*, vol. 51, no. 12, pp. 4203–4215, Dec. 2005.

[24] T. Gou and S. A. Jafar, "Degrees of freedom of the $K$ user $M \times N$ MIMO interference channel," *IEEE Transactions on Information Theory*, vol. 56, no. 12, pp. 6040–6057, Dec. 2010.

[25] S. W. Peters and R. W. Heath, Jr., "User partitioning for less overhead in MIMO interference channels," *IEEE Transactions on Wireless Communications*, vol. 11, no. 2, pp. 592–603, Feb. 2012.

[26] A. Lozano, R. W. Heath, Jr., and J. G. Andrews, "Fundamental limits of cooperation," submitted to *IEEE Transactions on Information Theory*, 2012. [Online]. Available: http://arxiv.org/pdf/1204.0011v1.pdf

[27] F. Baccelli and B. Blaszczyszyn, *Stochastic Geometry and Wireless Networks, Part II: Applications*, ser. Foundations and trends in networking. Now Publishers, 2009.

[28] S. P. Weber, X. Yang, J. G. Andrews, and G. de Veciana, "Transmission capacity of wireless ad hoc networks with outage constraints," *IEEE Transactions on Information Theory*, vol. 51, no. 12, pp. 4091–4102, Dec. 2005.

[29] S. Weber, J. G. Andrews, and N. Jindal, "An overview of the transmission capacity of wireless networks," *IEEE Transactions on Communications*, vol. 58, no. 12, pp. 3593–3604, Dec. 2010.

[30] D. Stoyan, W. S. Kendall, and J. Mecke, *Stochastic Geometry and Its Applications*, ser. Wiley-interscience paperback. John Wiley & Sons, 2008.

[31] R. K. Ganti and M. Haenggi, "Interference and outage in clustered wireless ad hoc networks," *IEEE Transactions on Information Theory*, vol. 55, no. 9, pp. 4067–4086, Sept. 2009.

[32] S. W. Peters and R. W. Heath, Jr., "Cooperative algorithms for MIMO interference channels," *IEEE Transactions on Vehicular Technology*, vol. 60, no. 1, pp. 206–218, Jan. 2011.

[33] G. Caire, N. Jindal, M. Kobayashi, and N. Ravindran, "Multiuser MIMO achievable rates with downlink training and channel state feedback," *IEEE Transactions on Information Theory*, vol. 56, no. 6, pp. 2845–2866, June 2010.

[34] C. Wang, E. K. S. Au, R. D. Murch, W. H. Mow, R. S. Cheng, and V. Lau, "On the performance of the MIMO zero-forcing receiver in the presence of channel estimation error," *IEEE Transactions on Wireless Communications*, vol. 6, no. 3, pp. 805–810, Mar. 2007.

[35] L. Musavian, M. R. Nakhai, M. Dohler, and A. H. Aghvami, "Effect of channel uncertainty on the mutual information of MIMO fading channels," *IEEE Transactions on Vehicular Technology*, vol. 56, no. 5, pp. 2798–2806, Sept. 2007.

[36] M. Kobayashi, N. Jindal, and G. Caire, "Training and feedback optimization for multiuser MIMO downlink," *IEEE Transactions on Communications*, vol. 59, no. 8, pp. 2228–2240, Aug. 2011.

[37] O. El Ayach and R. W. Heath, Jr., "Interference alignment with analog channel state feedback," *IEEE Transactions on Wireless Communications*, vol. 11, no. 2, pp. 626–636, Feb. 2012.

[38] B. Nosrat-Makouei, J. G. Andrews, and R. W. Heath, Jr., "MIMO interference alignment over correlated channels with imperfect CSI," *IEEE Transactions on Signal Processing*, vol. 59, no. 6, pp. 2783–2794, June 2011.

[39] B. Nosrat-Makouei, "Designing MIMO interference alignment networks," Ph.D. dissertation, The University of Texas at Austin, 2012.

[40] B. Nosrat-Makouei, K. G. Ganti, J. G. Andrews, and R. W. Heath, Jr., "MIMO interference alignment in random access networks," submitted to *IEEE Transactions on Communications*, 2012. [Online]. Available: http://arxiv.org/abs/1207.4254

[41] ——, "MIMO interference alignment in random access networks," in *Proc. 45th Asilomar Conference on Signals, Systems and Computers*, Pacific Grove, CA, Nov. 2011.

[42] S. P. Boyd and L. Vandenberghe, *Convex Optimization*. Cambridge Univ Pr, 2004.

[43] N. Jindal and A. Lozano, "A unified treatment of optimum pilot overhead in multipath fading channels," *IEEE Transactions on Communications*, vol. 58, no. 10, pp. 2939–2948, Oct. 2010.

[44] O. El Ayach, S. Peters, and R. W. Heath, Jr., "The practical challenges of interference alignment," *IEEE Wireless Communications*, vol. 20, no. 1, pp. 35–42, 2013.

[45] R. Tresch and M. Guillaud, "Cellular interference alignment with imperfect channel knowledge," *in Proc. of IEEE Intl. Conf. on Communications*, pp. 1–5, 2009.

[46] ——, "Clustered interference alignment in large cellular networks," *in Proc. of IEEE International Symposium on Personal, Indoor and Mobile Radio Communications*, pp. 1024–1028, 2009.

[47] M. Razaviyayn, M. Sanjabi, and Z.-Q. Luo, "Linear transceiver design for interference alignment: Complexity and computation," *IEEE Transactions on Information Theory*, vol. 58, no. 5, pp. 2896–2910, 2012.

[48] Q. Shi, M. Razaviyayn, Z.-Q. Luo, and C. He, "An iteratively weighted MMSE approach to distributed sum-utility maximization for a MIMO interfering broadcast channel," *IEEE Transactions on Signal Processing*, vol. 59, no. 9, pp. 4331–4340, 2011.

[49] Q. Spencer, C. Peel, A. Swindlehurst, and M. Haardt, "An introduction to the multi-user MIMO downlink," *IEEE Communications Magazine*, vol. 42, no. 10, pp. 60–67, 2004.

[50] I. Santamaria, O. Gonzalez, R. W. Heath, Jr., and S. Peters, "Maximum sum-rate interference alignment algorithms for MIMO channels," *Proc. of IEEE Global Telecommunications Conference*, pp. 1–6, 2010.

[51] S. Peters and R. W. Heath, Jr., "Cooperative algorithms for MIMO interference channels," *IEEE Trans. Veh. Technol.*, vol. 60, no. 1, pp. 206–218, 2011.

[52] R. W. Heath, Jr., T. Wu, Y. H. Kwon, and A. Soong, "Multiuser MIMO in Distributed Antenna Systems With Out-of-Cell Interference," *IEEE Trans. Signal Process.*, vol. 59, no. 10, pp. 4885–4899, 2011.

[53] S. Schwarz, R. W. Heath, and M. Rupp, "Single-user MIMO versus multi-user MIMO in distributed antenna systems with limited feedback," *EURASIP Journal on Advances in Signal Processing*, vol. 2013, no. 1, p. 54, 2013.

[54] D. Love and R. Heath Jr, "Equal gain transmission in multiple-input multiple-output wireless systems," *IEEE Trans. on Communications*, vol. 51, no. 7, pp. 1102–1110, 2003.

[55] S. Sesia, I. Toufik, and M. Baker, *LTE: the UMTS long term evolution*. Wiley Online Library, 2009.

[56] W. Yu and T. Lan, "Transmitter optimization for the multi-antenna downlink with per-antenna power constraints," *IEEE Transactions on Signal Processing*, vol. 55, no. 6, pp. 2646–2660, 2007.

[57] F. Boccardi and H. Huang, "Zero-forcing precoding for the MIMO broadcast channel under per-antenna power constraints," *in Proc. of IEEE 7th Workshop on Signal Processing Advances in Wireless Communications*, pp. 1–5, 2006.

[58] M. Vu, "MISO capacity with per-antenna power constraint," *IEEE Transactions on Communications*, vol. 59, no. 5, pp. 1268–1274, 2011.

[59] J. Starr, O. El Ayach, and R. W. Heath, Jr., "Interference alignment with per-antenna power constraints," *in Proc. of IEEE International Symposium on Information Theory Proceedings (ISIT)*, pp. 2746–2750, 2011.

[60] C. Yetis, T. Gou, S. Jafar, and A. Kayran, "On feasibility of interference alignment in MIMO interference networks," *IEEE Trans. Signal Process.*, vol. 58, no. 9, pp. 4771–4782, 2010.

[61] O. Gonzalez, C. Beltrán, and I. Santamaría, "On the feasibility of interference alignment for the K-user MIMO channel with constant coefficients," *arXiv preprint arXiv:1202.0186*, 2012.

[62] M. Razaviyayn, G. Lyubeznik, and Z.-Q. Luo, "On the degrees of freedom achievable through interference alignment in a MIMO interference channel," *IEEE Transactions on Signal Processing*, vol. 60, no. 2, pp. 812–821, 2012.

[63] G. Bresler, D. Cartwright, and D. Tse, "Settling the feasibility of interference alignment for the MIMO interference channel: the symmetric square case," *arXiv preprint arXiv:1104.0888*, 2011.

[64] K. Gomadam, V. R. Cadambe, and S. A. Jafar, "A distributed numerical approach to interference alignment and applications to wireless interference networks," *IEEE Transactions on Information Theory*, vol. 57, no. 6, pp. 3309–3322, 2011.

[65] O. El Ayach and R. W. Heath, Jr., "Interference alignment with analog channel state feedback," *IEEE Transactions on Wireless Communications*, vol. 11, no. 2, pp. 626–636, 2012.

[66] J. Thukral and H. Bolcskei, "Interference alignment with limited feedback," *Proc. IEEE International Symposium on Information Theory*, pp. 1759–1763, Jun. 28-Jul. 3 2009.

[67] R. Blum, "MIMO capacity with interference," *IEEE J. Sel. Areas Commun.*, vol. 21, no. 5, pp. 793–801, 2003.

[68] B. Nosrat-Makouei, J. Andrews, and R. W. Heath, Jr., "MIMO Interference Alignment Over Correlated Channels with Imperfect CSI," *IEEE Trans. Signal Process.*, vol. 59, no. 6, pp. 2783 –2794, 2010.

[69] J. Starr, O. El Ayach, and R. W. Heath, Jr., "Interference alignment in distributed antenna systems," *submitted to IEEE Transactions on Wireless Communications*, April 2013.

[70] O. El Ayach, A. Lozano, and R. W. Heath, Jr., "On the overhead of interference alignment: Training, feedback, and cooperation," *IEEE Transactions on Wireless Communications*, vol. 11, no. 11, pp. 4192–4203, 2012.

[71] S. Gollakota, S. Perli, and D. Katabi, "Interference alignment and cancellation," *Proc., ACM Conf. on Data Comm.*, pp. 159–170, 2009.

[72] O. El Ayach, S. W. Peters, and R. W. Heath, Jr., "The feasibility of interference alignment over measured MIMO-OFDM channels," *IEEE Transactions on Vehicular Technology*, vol. 59, no. 9, pp. 4309–4321, Nov. 2010.

[73] O. González, D. Ramirez, I. Santamaria, J. Garcia-Naya, and L. Castedo, "Experimental validation of Interference Alignment techniques using a multiuser MIMO testbed," *Proc., IEEE Intl. ITG Workshop on Smart Antennas*, pp. 1–8, 2011.

[74] T. Tang and R. Heath, "A space time receiver with joint synchronization and interference cancellation in asynchronous mimo-ofdm systems," *Vehicular Technology, IEEE Transactions on*, vol. 57, no. 5, pp. 2991–3005, 2008.

[75] H. Rahul, H. Hassanieh, and D. Katabi, "Sourcesync: a distributed wireless architecture for exploiting sender diversity," *SIGCOMM Comput. Commun. Rev.*, vol. 41, no. 4, pp. – , Aug. 2010. [Online]. Available: http://dl.acm.org/citation.cfm?id=2043164.1851204

[76] H. S. Rahul, S. Kumar, and D. Katabi, "Jmb: scaling wireless capacity with user demands," *SIGCOMM Comput. Commun. Rev.*, vol. 42, no. 4, pp. 235–246, Aug. 2012. [Online]. Available: http://doi.acm.org/10.1145/2377677.2377722

[77] H. V. Balan, R. Rogalin, A. Michaloliakos, K. Psounis, and G. Caire, "Airsync: Enabling distributed multiuser mimo with full spatial multiplexing," *Networking, IEEE/ACM Transactions on*, vol. PP, no. 99, pp. 1–1, 2013.

[78] D. J. Love, R. W. Heath, Jr., and T. Strohmer, "Grassmannian beamforming for multiple-input multiple-output wireless systems," *IEEE Transactions on Information Theory*, vol. 49, no. 10, pp. 2735–2747, Oct. 2003.

[79] S. W. Peters and R. W. Heath, Jr., "Interference alignment via alternating minimization," in *Proc. IEEE International Conference on Acoustics, Speech and Signal Processing*, Taipei, Taiwan, Apr. 2009, pp. 2445–2448.

[80] T. Schmidl and D. Cox, "Robust frequency and timing synchronization for ofdm," *Communications, IEEE Transactions on*, vol. 45, no. 12, pp. 1613–1621, 1997.

[81] *802.11N Draft STANDARD for Information Technology Telecommunications and information exchange between systems Local and metropolitan area networks Specific requirements*, Std.

[82] National Instruments. (2012) NI USRP 2921 Data Sheet. [Online]. Available: http://arxiv.org/pdf/0908.2282v1.pdf

[83] National Instruments. (2012) NI LabVIEW - Improving the Productivity of Engineers and Scientists. [Online]. Available: http://www.ni.com/labview/

[84] National Instruments. (2012) GPS Disciplined Oscillator (GPSDO) Kit Data Sheet. [Online]. Available: https://www.ettus.com/content/files/gpsdo-kit4.pdf